

N₂ fixation in the Mediterranean Sea related to the composition of the diazotrophic community, and impact of dust under present and future environmental conditions

Céline Ridame¹, Julie Dinasquet^{2,3}, Søren Hallstrøm⁴, Estelle Bigeard⁵, Lasse Riemann⁴, France Van Wambeke⁶, Matthieu Bressac⁷, Elvira Pulido-Villena⁶, Vincent Taillandier⁷, Frédéric Gazeau⁷, Antonio Tovar-Sanchez⁸, Anne-Claire Baudoux⁵, Cécile Guieu⁷

¹ Sorbonne University, CNRS, IRD, LOCEAN: Laboratoire d'Océanographie et du Climat: Expérimentation et Approches Numériques, UMR 7159, 75252 Paris Cedex 05, France

² Scripps Institution of Oceanography, University of California San Diego, USA

³ Sorbonne University, CNRS, Laboratoire d'Océanographie Microbienne, LOMIC, 66650 Banyuls-sur-Mer, France

⁴ Marine Biology Section, Department of Biology, University of Copenhagen, 3000 Helsingør, Denmark

⁵ Sorbonne University, CNRS, Station Biologique de Roscoff, UMR 7144 Adaptation et Diversité en Milieu Marin, France

⁶ Aix-Marseille Université, Université de Toulon, CNRS/INSU, IRD, Mediterranean Institute of Oceanography (MIO), UM 110, 13288, Marseille, France

⁷ Sorbonne Université, CNRS, Laboratoire d'Océanographie de Villefranche, LOV, 06230 Villefranche-sur-Mer, France

⁸ Department of Ecology and Coastal Management, Institute of Marine Sciences of Andalusia (CSIC), 11510 Puerto Real, Cádiz, Spain

Correspondence to: Céline Ridame (celine.ridame@locean.ipsl.fr)

Abstract. N₂ fixation rates were measured in the 0-1000 m layer at 13 stations located in the open western and central Mediterranean Sea (MS) during the PEACETIME cruise (late spring 2017). While the spatial variability of N₂ fixation was not related to Fe, P nor N stocks, the surface composition of the diazotrophic community indicated a strong longitudinal gradient increasing eastward for the relative abundance of non-cyanobacterial diazotrophs (NCD) (mainly γ -Proteobacteria) and conversely decreasing eastward for UCYN-A (mainly -A1 and -A3) as did N₂ fixation rates. UCYN-A4 and -A3 were identified for the first time in the MS. The westernmost station influenced by Atlantic waters, and characterized by highest stocks of N and P, displayed a patchy distribution of diazotrophic activity with an exceptionally high rate in the euphotic layer of 72.1 nmol N L⁻¹ d⁻¹, which could support up to 19 % of primary production. At this station at 1%PAR depth, UCYN-A4 represented up to 94 % of the diazotrophic community. These *in situ* observations of greater relative abundance of UCYN-A at stations with higher nutrient concentrations and dominance of NCD at more oligotrophic stations suggest that nutrient conditions - even in the nanomolar range - may determine the composition of diazotrophic communities and in turn N₂ fixation rates. The impact of Saharan dust deposition on N₂ fixation and diazotrophic communities was also investigated, under present and future projected conditions of temperature and pH during short term (3-4 days) experiments at three

35 stations. New nutrients from simulated dust deposition triggered a significant stimulation of N₂ fixation (from 41 % to 565
36 %). The strongest increase in N₂ fixation was observed at the stations dominated by NCD and did not lead on this short time
37 scale to change in the diazotrophic community composition. Under projected future conditions, N₂ fixation was either
38 increased or unchanged; in that later case this was probably due to a too low nutrient bioavailability or an increased grazing
39 pressure. The future warming and acidification likely benefited NCD (*Pseudomonas*) and UCYN-A2 while disadvantaged
40 UCYN-A3 without knowing which effect (alone or in combination) is the driver, especially since we do not know the
41 temperature optima of these species not yet cultivated as well as the effect of acidification.

42 **1. Introduction**

43 The Mediterranean Sea (MS) is considered as one of the most oligotrophic regions of the world's ocean (Krom et al., 2004;
44 Bosc et al., 2004). It is characterized by a longitudinal gradient in nutrient availability, phytoplanktonic biomass and primary
45 production (PP) decreasing eastward (Manca et al., 2004; D'Ortenzio and Ribera d'Alcalà, 2009; Ignatiades et al., 2009;
46 Siokou-Frangou et al., 2010; El Hourany et al., 2019). From May to October, the upper water column is well-stratified
47 (D'Ortenzio et al., 2005), and the sea surface mixed layer (SML) becomes nutrient-depleted leading to low PP (e.g. Lazzari
48 et al., 2012). Most measurements of N₂ fixation during the stratified period have shown low rates ($\leq 0.5 \text{ nmol N L}^{-1} \text{ d}^{-1}$) in
49 surface waters of the open MS (Ibello et al., 2010; Bonnet et al., 2011; Yogeve et al., 2011; Ridame et al., 2011; Rahav et al.,
50 2013a; Benavides et al., 2016) indicating that N₂ fixation represents a minor source of bioavailable nitrogen in the MS
51 (Krom et al., 2010; Bonnet et al., 2011). These low rates are likely related to the extremely low bioavailability in dissolved
52 inorganic phosphorus (DIP) (Rees et al., 2006; Ridame et al., 2011). The high concentrations of dissolved iron (DFe) in the
53 SML due to accumulated atmospheric Fe deposition (Bonnet and Guieu 2006; Tovar-Sánchez et al. 2020; Bressac et al.,
54 2021), suggest that the bioavailability of Fe is not a controlling factor of N₂ fixation (Ridame et al., 2011). Occasionally,
55 high N₂ fixation rates have been reported locally in the northwestern ($17 \text{ nmol N L}^{-1} \text{ d}^{-1}$; Garcia et al., 2006) and eastern MS
56 ($129 \text{ nmol N L}^{-1} \text{ d}^{-1}$; Rees et al., 2006). Usually, the low N₂ fixation rates in the Mediterranean offshore waters are associated
57 with low abundance of diazotrophs, mainly dominated by unicellular organisms (Man-Aharonovich et al., 2007; Yogeve et
58 al., 2011; Le Moal et al., 2011). Unicellular diazotrophs from the photo-heterotrophic group A (UCYN-A, Zehr et al., 1998)
59 largely dominated the cyanobacteria assemblage in the MS (Le Moal et al., 2011), and very low concentrations of
60 filamentous diazotrophic cyanobacteria have only been recorded in the eastern basin (Bar-Zeev et al., 2008; Le Moal et al.,
61 2011; Yogeve et al., 2011). The UCYN-A cluster consist of four sublineages: UCYN-A1, -A2, -A3 and -A4 (Thompson et al.,
62 2014; Farnelid et al., 2016; Turk Kubo et al., 2017; Cornejo-Castillo et al., 2019), of which only UCYN-A1 and -A2 have
63 been previously detected in the MS (Man-Aharonovich et al., 2007; Martinez-Perez et al., 2016; Pierrela Karlusich et al.,
64 2021). Heterotrophic diazotrophs are widely distributed over the offshore surface waters (Le Moal et al, 2011), and the
65 decreasing eastward gradient of surface N₂ fixation rate could be related to a predominance of photo-autotrophic diazotrophs
66 in the western basin and a predominance of heterotrophic diazotrophs in the eastern one (Rahav et al. 2013a).

67 The MS is strongly impacted by periodic dust events, originating from the Sahara, which have been recognized as a
68 significant source of macro- and micronutrients, to the nutrient depleted SML during stratified periods (Guieu and Ridame,
69 2020 and references therein; Mas et al., 2020). Results from Saharan dust seeding experiments during open sea microcosms
70 and coastal mesocosms in the MS, showed stimulation of both PP (Herut et al., 2005; Ternon et al., 2011; Ridame et al.,
71 2014 ; Herut et al., 2016) and heterotrophic bacterial production (BP) (Pulido-Villena et al., 2008, 2014; Lekunberri et al.,
72 2010; Herut et al., 2016). Experimental Saharan dust seeding was also shown to enhance N₂ fixation in the western and
73 eastern MS (Ridame et al., 2011; Ternon et al., 2011; Ridame et al., 2013; Rahav et al., 2016a) and to alter the composition
74 of the diazotrophic community (Rahav et al., 2016a), as also shown in the tropical North Atlantic (Langlois et al., 2012).

75 The MS has been identified as one of the primary hot-spots for climate change (Giorgi, 2006). Future sea surface warming
76 and associated increase in stratification (Somot et al., 2008) might reinforce the importance of atmospheric inputs as a source
77 of new nutrients for biological activities during that season, including diazotrophic microorganisms. This fertilizing effect
78 could also be enhanced by the expected decline in pH (Mermex Group, 2011), which could increase the nutrient dust
79 solubility in seawater. Under nutrient depleted conditions, predicted elevated temperature and CO₂ concentration favor the
80 growth and N₂ fixation of the filamentous cyanobacteria *Trichodesmium* and of the photo-autotrophic UCYN-B and -C
81 (Webb et al., 2008; Hutchins et al., 2013; Fu et al., 2008, 2014; Eichner et al., 2014; Jiang et al., 2018), whereas effects on
82 UCYN-A and non-cyanobacterial diazotrophs (NCD) are uncertain.

83 In this context, the first objective of this study is to investigate during the season characterized by strong stratification and
84 low productivity, the spatial variability of N₂ fixation rates in relation to nutrient availability and diazotrophic community
85 composition. The second objective was to study, for the first time, the impact of a realistic Saharan deposition event in the
86 open MS, on N₂ fixation rates and diazotrophic communities composition under present and realistic projected conditions of
87 temperature and pH for 2100.

88

89 **2. Materials and Methods**

90 **2.1 Oceanographic cruise**

91 All data were acquired during the PEACETIME cruise (ProcEss studies at the Air-sEa Interface after dust deposition in the
92 MEiterranean sea) in the western and central MS on board the R/V *Pourquoi Pas ?* from May 10 to June 11, 2017
93 (<http://peacetime-project.org/>) (see the detailed description in Guieu et al., 2020). The cruise track including ten short
94 stations (ST1 to ST10) and three long stations (TYR, ION and FAST) is shown in Fig.1 (coordinates in Table S1). Stations 1
95 and 2 were located in the Liguro-Provencal basin; Stations 5, 6, and TYR, in the Tyrrhenian Sea; Stations 7, 8, and ION in
96 the Ionian Sea; and Stations 3, 4, 9, 10 and FAST in the Algerian basin.

97

98 **2.2 Dust seeding experiments**

99 Experimental dust seedings into six large tanks were conducted at each of the three long stations (TYR, ION and FAST),
100 under present and future conditions of temperature and pH. Based on previous studies, the location of these stations was

101 chosen based on several criteria including because they represent three main bioregions of the MS (Guieu et al., 2020, their
102 Fig. S1). They are located along the longitudinal gradient in biological activity, including the activity of diazotrophs
103 decreasing eastward (Bonnet et al., 2011; Rahav et al., 2013a). The experimental setup is fully described in a companion
104 paper (Gazeau et al., 2021a). Briefly, six climate reactors (volume of about 300 L) made in high density polyethylene were
105 placed in a temperature-controlled container, and covered with a lid equipped with LEDs to reproduce natural light cycle.
106 The tanks were filled with unfiltered surface seawater collected at ~5m with a peristaltic pump at the end of the day (T-12h)
107 before the start of the experiments the next morning (T0). Two replicate tanks were amended with mineral Saharan dust
108 (Dust treatments D1 and D2) simulating a high but realistic atmospheric dust deposition of 10 g m^{-2} (Guieu et al., 2010b).
109 Two other tanks were also amended with Saharan dust (same dust flux as in the Dust treatment) under warmer ($\sim +3^\circ \text{ C}$) and
110 more acidic water conditions (~ -0.3 pH unit) (Greenhouse treatments G1 and G2). This corresponds to the IPCC projections
111 for 2100 under RCP8.5 (IPCC 2019). Seawater in G1 and G2 was warmed overnight to reach $+3^\circ \text{ C}$ and acidified through
112 the addition of CO_2 -saturated $0.2 \text{ }\mu\text{m}$ -filtered seawater ($\sim 1.5 \text{ L}$ in 300 L). The difference in temperature between G
113 (Greenhouse) tanks and other tanks (C, Controls and D, Dust) was $+3^\circ \text{ C}$, $+3.2^\circ \text{ C}$ and $+3.6^\circ \text{ C}$ at TYR, ION and FAST,
114 respectively, and the decrease in pH was -0.31 , -0.29 and -0.33 at TYR, ION and FAST, respectively (Gazeau et al., 2021a).
115 Two tanks were filled with untreated water (Controls C1 and C2). The experiment at TYR and ION lasted three days while
116 the experiment at FAST lasted four days. The sampling session took place every morning at the same time over the duration
117 of the experiments.

118 The fine fraction ($< 20 \text{ }\mu\text{m}$) of a Saharan soil collected in southern Tunisia used in this study, has been previously used for
119 the seeding of mesocosms in the frame of the DUNE project (a DUst experiment in a low-Nutrient, low-chlorophyll
120 Ecosystem). Briefly, the dust was previously subjected to physico-chemical transformations mimicking the mixing between
121 dust and pollution air masses during atmospheric transport (see details in Desboeufs et al, 2001; Guieu et al., 2010b). This
122 dust contained $0.055 \pm 0.003 \%$ of P, $1.36 \pm 0.09 \%$ of N, and $2.26 \pm 0.03 \%$ of Fe, in weight (Desboeufs et al., 2014). Right
123 before the artificial seeding, the dust was mixed with 2 L of ultrapure water in order to mimic a wet deposition event and
124 sprayed at the surface of the climate reactors D and G. The succession of operations is fully described in Gazeau et al.,
125 (2021a, see their Table 1).

126

127 **2.3 N_2 fixation and primary production**

128 All materials were acid washed (HCl Suprapur 32%) following trace metal clean procedures. Before sampling, bottles were
129 rinsed three times with the sampled seawater. For the *in situ* measurements, seawater was sampled using a trace metal clean
130 (TMC) rosette equipped with 24 GO-FLO Bottles (Guieu et al., 2020). At each station, 7 to 9 depths were sampled between
131 surface and 1000 m for N_2 fixation measurements, and 5 depths between surface and $\sim 100 \text{ m}$ for primary production
132 measurements (one sample par depth). During the seeding experiments, the six tanks were sampled for simultaneous
133 determination of N_2 - and CO_2 net fixation rates before dust seeding (initial time T0) and one day (T1), two days (T2), and

134 three days (T3) after dust addition at TYR and ION Stations. At FAST, the last sampling took place four days (T4) after dust
135 addition.

136 After collection, 2.3 L of seawater were immediately filtered onto pre-combusted GFF filters to determine natural
137 concentrations and isotopic signatures of particulate organic carbon (POC) and particulate nitrogen (PN). Net N₂ fixation
138 rates were determined using the ¹⁵N₂ gas-tracer addition method (Montoya et al., 1996), and net primary production using the
139 ¹³C-tracer addition method (Hama et al., 1983). Immediately after sampling, 1 mL of NaH¹³CO₃ (99 %, Eurisotop) and 2.5
140 ml of 99 % ¹⁵N₂ (Eurisotop) were introduced to 2.3 L polycarbonate bottles through a butyl septum for simultaneous
141 determination of N₂- and CO₂-fixation. ¹⁵N₂ and ¹³C tracers were added to obtain a ~10 % final enrichment. Then, each bottle
142 was vigorously shaken before incubation for 24 h. The *in situ* samples from the euphotic zone were incubated in on-deck
143 containers with circulating seawater, equipped with blue filters with different sets of blue neutral density filters (Lee Filters)
144 (percentages of attenuation: 70, 52, 38, 25, 14, 7, 4, 2 and 1 %) to simulate an irradiance level (% PAR) as close as possible
145 to the one corresponding to their depth of origin. Samples for N₂ fixation determination in the aphotic layer were incubated
146 in the dark in thermostated incubators set at *in situ* temperature. *In situ* ¹³C-PP will not be discussed in this paper as ¹⁴C-PP
147 rates are presented in Maranon et al. (2021) (see details in Fig. S1). The *in situ* ¹³C-PP and molar C/N ratio in the organic
148 particulate matter, measured simultaneously in our samples (see below for details), were used to estimate the contribution of
149 N₂ fixation to PP.

150 Samples from the dust addition experiments were incubated in two tanks dedicated to incubation: one tank at the same
151 temperature and irradiance as tanks C and D, and another one at the same temperature and irradiance as tanks G. It should be
152 noted that ¹⁴C-PP was also measured during the seedings experiments (Gazeau et al., 2021b).

153 After 24 h incubation, 2.3 L were filtered onto pre-combusted 25 mm GF/F filters, and filters were stored at -25° C. Filters
154 were then dried at 40° C for 48 h before analysis. POC and PN as well as ¹⁵N and ¹³C isotopic ratios were quantified using an
155 online continuous flow elemental analyzer (Flash 2000 HT), coupled with an Isotopic Ratio Mass Spectrometer (Delta V
156 Advantage via a conflow IV interface from Thermo Fischer Scientific). For each sample, POC (in the 0-100m layer) and PN
157 (0-1000m) were higher than the analytically determined detection limit of 0.15 μmol for C and 0.11 μmol for N. Standard
158 deviations were 0.0007 atom% and 0.0005 atom% for ¹³C and ¹⁵N enrichment, respectively. The atom% excess of the
159 dissolved inorganic carbon (DIC) was calculated by using measured DIC concentrations at the LOCEAN laboratory
160 (SNAPO-CO₂). N₂ fixation rates were calculated by isotope mass balance equations as described by Montoya et al. (1996).
161 For each sample, the ¹³C and ¹⁵N uptake rates were considered as significant when excess enrichment of POC and PN was
162 greater than three times the standard deviation obtained on natural samples. According to our experimental conditions, the
163 minimum detectable ¹³C and ¹⁵N uptake rates in our samples were 5 nmol C L⁻¹ d⁻¹ and 0.04 nmol N L⁻¹ d⁻¹, respectively.
164 CO₂ uptake rates were above the detection limit in the upper 0-100m, while N₂ fixation was not quantifiable below 300 m
165 depth except at Stations 1 and 10 with rates ~0.05 nmol N L⁻¹ d⁻¹ at 500 m depth. From these measurements, the molar C:N
166 ratio in the organic particulate matter was calculated and used to estimate the contribution of N₂ fixation to primary
167 production. As a rough estimate of the potential impact of bioavailable N input from N₂ fixation on BP, we used the BP rates

168 presented in companion papers (Gazeau et al., 2021b; Van Wambeke et al., 2021), and converted them in N demand using
169 the molar ratio C/N of 6.8 (Fukuda et al., 1998). Trapezoidal method was used to calculate integrated rates over the SML, the
170 euphotic layer (from surface to 1 % photosynthetically available radiation (PAR) depth) and the 0-1000 m water column.
171 It must be noted that N₂ fixation rates measured by the ¹⁵N₂-tracer gas addition method may have been underestimated due to
172 incomplete ¹⁵N₂ gas bubble equilibration (Mohr et al., 2010). However, this potential underestimation is strongly lowered
173 during long incubation (24h).

174 The relative changes (RC, in %) in N₂ fixation in the dust experiments were calculated as follows :

$$RC (\%) = 100 \times \frac{(N_2FIXATION_{Tx} - N_2FIXATION_{Control})}{(N_2FIXATION_{Control})}$$

175 with N₂ Fixation_{Tx} the rate in D1, D2, G1 or G2 at Tx, N₂ Fixation_{Control} the mean of the duplicated controls (C1 and C2) at
176 Tx, and Tx the time of the sampling.

177

178 **2.4 Composition of the diazotrophic community**

179 Samples for characterization of the diazotrophic communities were collected during the dust seeding experiments in the six
180 tanks at initial time before seeding (T0) and final time (T3 at TYR and ION, and T4 at FAST). Three liters of water were
181 collected in acid-washed containers from each tank, filtered onto 0.2 µm PES filters (Sterivex) and stored at -80° C until
182 DNA extraction. The composition of the diazotrophic community was also determined at four depths (10, 61, 88 and 200 m)
183 at Station 10. Here, 2 L seawater were collected from the TMC rosette. Immediately after collection, seawater was filtered
184 under low vacuum pressure through a 0.2 µm-Nuclepore membrane and stored at -80° C in cryovials. Nucleic acids were
185 obtained from both filter types using phenol-chloroform extraction followed by purification (NucleoSpin® PlantII kit;
186 Macherey-Nagel). DNA extracts were used as templates for PCR amplification of the nifH gene by nested PCR protocol as
187 fully described in Bigeard et al., (2021, protocol.io). Following polymerase chain reactions, DNA amplicons were purified,
188 and quantified using NanoQuant Plate™ and Tecan Spark® (Tecan Trading AG, Switzerland). Each PCR product was
189 normalized to 30ng/µl in final 50µl and sent to Genotoul (<https://www.genotoul.fr/>, Toulouse, France) for high throughput
190 sequencing using paired-end 2x250bp Illumina MiSeq. All reads were processed using the Quantitative Insight Into
191 Microbial Ecology 2 pipeline (QIIME2 v2020.2, Bolyen et al., 2019). Reads were truncated to 350 bp based on sequencing
192 quality, denoised, merged and chimera-checked using DADA2 (Callahan et al., 2016). A total of 1,029,778 reads were
193 assigned to 635 amplicon sequence variants (ASVs). The table was rarefied by filtering at 1 % relative abundance per sample
194 cut-off that reduced the dataset to 97 ASVs accounting for 98.27 % of all reads. Filtering for homologous genes was done
195 using the NifMAP pipeline (Angel et al., 2018) and translation into amino acids using FrameBot (Wang et al., 2013). This
196 yielded 235 ASVs accounting for 1,022,184 reads (99 %). These remaining ASVs were classified with DIAMOND blastp
197 (Buchfink et al 2015) using a FrameBot translated nifH database (phylum level version; Moynihan, 2020) based on the ARB
198 database from the Zehr Lab (version June 2017; <https://www.jzehrlab.com/nifh>). NifH cluster and subcluster designations
199 were assigned according to Frank et al. (2016). UCYN-A sublineages were assigned by comparison to UCYN-A reference

200 sequences (Farnelid et al., 2016; Turk-Kubo et al., 2017). All sequences associated with this study have been deposited
201 under the BioProject ID: PRJNA693966. Alpha and beta-diversity indices for community composition, were estimated after
202 randomized subsampling. Analyses were run in QIIME 2 and in Primer v.6 software package (Clarke and Warwick, 2001).

204 **2.5 Complementary data from PEACETIME companions papers**

205 **Bacterial production-** Heterotrophic bacterial production (BP, *sensus stricto* referring to prokaryotic heterotrophic
206 production) was determined on board using the microcentrifuge method with the ^3H - leucine (^3H -Leu) incorporation
207 technique to measure protein production (Smith and Azam, 1992). The detailed protocol and the rates of BP are presented in
208 Van Wambeke et al. (2021) for measurements in the water column, and in Gazeau et al. (2021b) for measurements over the
209 course of the dust seeding experiments.

210 **Dissolved Fe-** Dissolved iron (DFe) concentrations ($< 0.2 \mu\text{m}$) were measured by flow injection analysis with online
211 preconcentration and chemiluminescence detection (FIA-CL). The detection limit was 15 pM (Bressac et al., 2021). DFe
212 concentrations in the water column along the whole transect are presented in Bressac et al. (2021) and for the dust seeding
213 experiments in Roy-Barman et al. (2021).

214 **Dissolved inorganic phosphorus and nitrate-** Concentrations of DIP and nitrate (NO_3^-) were analyzed immediately after
215 collection on $0.2 \mu\text{m}$ filtered seawater using a segmented flow analyzer (AAIII HR Seal Analytical) according to Aminot and
216 K  rouel (2007) with respective detection limits of $0.02 \mu\text{mol L}^{-1}$ and $0.05 \mu\text{mol L}^{-1}$. Samples with concentrations below the
217 limit of detection with standard analysis were analyzed by spectrophotometry using a 2.5 m long waveguide capillary cell
218 (LWCC) for DIP (Pulido-Villena et al., 2010) and a 1 m LWCC for NO_3^- (Louis et al., 2015); the limit of detection was 1
219 nM for DIP and 6 nM for NO_3^- . Samples for determination of NO_3^- at nanomolar level were lost from Stations 1 to 4. The
220 dust addition experiments data are detailed in Gazeau et al. (2021a). The water column data are fully discussed in Pulido-
221 Villena et al. (2021) and Van Wambeke et al. (2021).

223 **2.6 Statistical analysis**

224 Pearson's correlation coefficient was used to test the statistical linear relationship ($p < 0.05$) between N_2 fixation and other
225 variables (BP, PP, DFe, DIP, NO_3^-); it should be noted that the DIN stocks estimated at Stations 1 to 4 (Table S1) were
226 excluded from statistical analysis. In the dust seeding experiments, means at initial time (T0) before dust amendment
227 (average at T0 in C and D treatments; $n = 4$, see Table 2) were compared using a one-way ANOVA followed by a Tukey
228 means comparison test ($\alpha = 0.05$). When assumptions for ANOVA were not respected, means were compared using a
229 Kruskal–Wallis test and a post hoc Dunn test. To test significant differences ($p < 0.05$) between the slopes of N_2 fixation as a
230 function of time in the C, D and G treatments ($n = 8$), an Ancova was performed on data presenting a significant linear
231 relationship with time (Pearson's correlation coefficient, $p < 0.05$). Statistical tests were done using XLSTAT and R (version
232 4.1.1 with the stats, tidyverse and FactoMineR packages).

234 3. Results

235

236 3.1 *In situ* N₂ fixation

237 3.1.1 Vertical and longitudinal distribution of N₂ fixation

238 Over the cruise, the water column was well stratified with a shallow SML varying from 7 to 21 m depth (Table S1).
239 Detectable N₂ fixation rates in the 0-1000 m layer ranged from 0.04 to an exceptionally high rate of 72.1 nmol N L⁻¹ d⁻¹ at
240 Station 10 (Fig.2). Vertical N₂ fixation profiles exhibited a similar shape at all stations with maximum values within the
241 euphotic layer and undetectable values below 300 m depth (except at Stations 1 and 10 with rates ~ 0.05 nmol N L⁻¹ d⁻¹ at 500
242 m depth). Within the euphotic layer, all the rates were well above the detection limit (DL = 0.04 nmol N L⁻¹ d⁻¹; minimum *in*
243 *situ* N₂ fixation = 0.22 nmol N L⁻¹ d⁻¹). The highest rates were generally found below the SML and the lowest at the base of
244 the euphotic layer or within the SML (Fig.2). The lowest N₂ fixation rates integrated over the euphotic and aphotic (defined
245 as 1 % PAR depth to 1000 m) layers were found at Station 8, and the highest at Station 10 (Table 1). On average, 59 ± 16 %
246 of N₂ fixation (min 42 % at TYR and ION, max 97 % at Station 10) took place within the euphotic layer (Table 1). The
247 contribution of the SML integrated N₂ fixation to the euphotic layer integrated N₂ fixation was low, on average 17 ± 10 %.
248 Volumetric surface (~ 5 m) and euphotic layer integrated N₂ fixation rates exhibited a longitudinal gradient decreasing
249 eastward (r = -0.59 and r = -0.60, p < 0.05, respectively) (Fig.3). Integrated N₂ fixation rates over the SML, aphotic and 0-
250 1000 m layers (Table 1) displayed no significant trend with longitude (p > 0.05). It should be noted that longitudinal trends
251 with stronger correlations were observed for ¹³C-PP and BP (r = -0.81 and r = -0.82, p < 0.05, respectively, Fig.S2) as well as
252 DIP and NO₃⁻ stocks (r = -0.68 and r = -0.85, p < 0.05, no correlation with DFe stock; data not shown) integrated over the
253 euphotic layer.

254

255 3.1.2 N₂ fixation and composition of diazotrophs at Station 10

256 The westernmost Station 10 was in sharp contrast to all other stations with an euphotic integrated N₂ fixation on average 44
257 times higher (Table 1) due to high rates of 2.9 at 37 m and 72.1 nmol N L⁻¹ d⁻¹ at 61 m (i.e. at the deep chlorophyll-a
258 maximum, DCM) (Fig.2). That rate at 61 m was associated with a maximum in PP but not with a maximum in BP. From
259 surface to 200 m depth, the *nifH* community composition was largely dominated by ASVs related to different UCYN-A
260 groups (Fig.4) that represented 86 % at 200 m and up to 99.5 % at the DCM. No UCYN-B and -C or filamentous
261 diazotrophs were detected. The relative abundance of NCD (mainly γ-Proteobacteria *Pseudomonas*) increased with depth (r
262 = 0.96, p < 0.05) to reach about 8 % in the mesopelagic layer (200 m). UCYN-A1 and -A4 dominated the total diazotrophic
263 community (from 51 to 99 %). All four UCYN-A had different vertical distributions: the relative abundances of UCYN-A1
264 and -A3 were the highest in surface while UCYN-A4 was dominant at the most productive depths (61 and 88 m). At 61 m
265 depth, where the unusually high rate of N₂ fixation was detected, the community was dominated by both UCYN-A4 (58 %)
266 and UCYN-A1 (41 %).

267

268 **3.1.3 N₂ fixation versus primary production, heterotrophic bacterial production, nutrients**

269 For statistical analysis, due to the high integrated N₂ fixation rate from Station 10, this rate was not included in order not to
270 bias the analysis. N₂ fixation rate integrated over the euphotic layer correlated strongly with PP ($r = 0.71$, $p < 0.05$) and BP (r
271 $= 0.76$; $p < 0.05$) (Fig.5). Integrated N₂ fixation over the euphotic layer (and over the SML) was not correlated with the
272 associated DFe, DIP and NO₃⁻ stocks ($p > 0.05$). It should be noted that DIP and NO₃⁻ stocks correlated positively with PP
273 and BP ($p < 0.05$) over the euphotic layer (no correlation between DFe stock, and PP, BP).

275 **3.2 Response of N₂ fixation and composition of the diazotrophic communities to dust seeding**

276 **3.2.1 Initial characteristics of the tested seawater**

277 N₂ fixation and BP were the highest at FAST while PP was the highest at FAST and ION (Table 2). The N₂ fixation rates
278 were similar at ION and TYR and significantly higher (factor ~2.6) at FAST. At TYR and ION, the diazotrophs community
279 was largely dominated by NCD (on average 94.5 % of the total diazotrophic community) whereas at FAST, diazotrophic
280 cyanobacteria, mainly UCYN-A, represented on average 91.4 % of the total diazotrophic community. NO₃⁻ concentration
281 was the highest at FAST (59 nM) while DIP concentration was the highest at TYR (17 nM) and the lowest at ION (7 nM).
282 The molar NO₃⁻/DIP ratio was strongly lower than the Redfield ratio (16/1) indicating a potential N limitation of the
283 phytoplanktonic activity in all experiments. DFe concentrations were all higher than 1.5 nM.

285 **3.2.2 Changes in N₂ fixation in response to dust seeding and relationship with changes in primary and heterotrophic 286 bacterial production**

287 All the dust seedings led to a significant stimulation of N₂ fixation relative to the controls under present and future climate
288 conditions (D and G treatments) (Figs.6, S3). The reproducibility between the replicated treatments was good at all stations
289 (mean coefficient of variation (CV%) < 14 %). The maximum N₂ fixation relative change (RC) was the highest at TYR
290 (+434-503 % in D1 and D2, +478-565 % in G1 and G2) then at ION (+256-173 % in D1 and D2, and +261-217 % in G1 and
291 G2) and finally at FAST (+41-49 % in D1 and D2 and +97-120 % in G1 and G2) (Fig.7). At TYR and FAST, dust addition
292 stimulated N₂ fixation more in the G treatment than in D, whereas at ION the response was similar between the treatments
293 (Fig.S3). N₂ fixation measured during the dust seeding experiments correlated strongly with PP at FAST ($r = 0.90$, $p < 0.05$),
294 and with BP at TYR and ION ($r > 0.76$, $p < 0.05$) (Fig. S4).

295 **3.2.3 Changes in the diazotrophic composition in response to dust seeding**

296 At TYR and ION, the diazotrophic communities before seeding were largely dominated by NCD (~ 94.5 % of total ASVs,
297 Fig. 8, Table 2). These were mainly γ -proteobacteria related to *Pseudomonas*. Some of these ASVs had low overall relative
298 abundance, and therefore did not appear in the top 20 ASVs (Fig.8; Tables S2, S3) but could nevertheless, account for up to
299 16 % in a specific sample. Filamentous cyanobacteria (*Katagnymene*) were also observed at both stations (~ 4.7 % of the
300 total diazotrophs). The community at FAST was initially dominated by UCYN-A phylotypes, mostly represented by UCYN-

301 A1 and -A3 (relative abundance of UCYN-A1 and -A3 in C and D treatments at T0, n=4 : 34 ± 6 % and 45 ± 2 % of the total
302 diazotrophic composition, respectively, Fig.8). At TYR and ION, the variability at T0 between replicates was higher than at
303 FAST (Fig. S5; C1T0 at TYR was removed due to poor sequencing quality). Also, the diversity (Shannon H') was generally
304 higher at TYR and ION at the start of incubations compared to FAST (T0, Fig.S6). For ION and FAST experiments,
305 *Pseudomonas* related ASVs were more abundant in G treatments at T0 relative to Control and Dust treatments (T0). At the
306 end of the TYR and ION experiments, the community from all treatments appeared to converge (Fig.S5) due to the increase
307 of a few γ -proteobacteria (mainly *Pseudomonas*) that strongly increased in all treatments (Fig.8). At FAST, no difference in
308 the relative abundances of diazotrophs was recorded between D treatment and the controls at T4. However, when comparing
309 G treatment relative to D at T4, the relative contribution of NCD was higher (82 % in G vs. 63 % in D) and the relative
310 abundance of UCYN-A was lower (13 % in G vs. 31 % in D).

311

312 **4. Discussion**

313 Late spring, at the time of sampling, all the stations were well-stratified and characterized by oligotrophic conditions
314 increasing eastward (Maranon et al., 2021; Fig.8 in Guieu et al., 2020). NO_3^- and DIP concentrations were low in the SML,
315 from 9 to 135 nM for NO_3^- (Van Wambeke et al., 2021) and from 4 to 17 nM for DIP (Pulido-Villena et al., 2021); the
316 highest stocks were measured at the westernmost station (St 10) (Table S1).

317

318 **4.1 General features in N_2 fixation and diazotroph community composition**

319 N_2 fixation rates in the aphotic layer were in the range of those previously measured in the western open MS (Benavides et
320 al., 2016) and accounted, on average, for 41 % of N_2 fixation in the 0-1000 m layer, suggesting that a large part of the total
321 diazotrophic activity was related to heterotrophic NCD in the aphotic layer. N_2 fixation rates in the euphotic layer were of the
322 same order of magnitude (data from St10 excluded) than those previously measured in the open MS in spring and summer
323 (Bonnet et al., 2011; Rahav et al., 2013a). At the tested stations, the surface diazotrophic cyanobacteria were largely
324 dominated by UCYN-A (~ 93 % of the total diazotrophic cyanobacteria, mostly UCYN-A1 and -A3) and the NCD
325 community by γ -proteobacteria (~ 95 % of the total NCD). This is the first time that UCYN-A3 and -A4 are detected in the
326 MS. The photo-autotrophic N_2 fixation was negligible as no UCYN-B and -C were detected and very low abundance of
327 filamentous cyanobacteria was observed.

328

329 **4.2 Longitudinal gradient of N_2 fixation related to the composition of the diazotrophic communities**

330 At Station 10 and FAST, the surface diazotrophic communities were largely dominated by UCYN-A (> 91 %) whereas at
331 TYR and ION they were dominated by NCD (> 94 %) which highlights the predominance of photo-heterotrophic
332 diazotrophy in the western waters of the Algerian Basin and of NCD-supported diazotrophy in the Tyrrhenian and Ionian
333 basins. Surface N_2 fixation exhibited a longitudinal gradient decreasing eastward as previously reported (Bonnet et al., 2011,
334 Rahav et al., 2013a). Strong longitudinal gradients decreasing eastward for the relative abundance of UCYN-A ($r = -0.93$, p

335 < 0.05) and inversely increasing eastward for NCD were observed ($r = 0.89$, $p < 0.05$) (Fig.9). Despite no quantitative
336 abundances of distinct diazotrophs for the studied area (in this and previously published studies), the intensity of the bulk N_2
337 fixation rate was likely related to the overall composition of the diazotrophic communities (here relative abundance of
338 UCYN-A versus NCD). Indeed, surface N_2 fixation rates correlated positively with the relative abundance of UCYN-A
339 (mainly A1 and A3) ($r = 0.98$, $p < 0.05$) and negatively with the relative abundance of NCD ($r = -0.99$, $p < 0.05$) (Fig. S7).
340 This could be related, in part, to the variability of the cell-specific N_2 fixation rates that were shown to be higher for UCYN-
341 A relative to NCD (Turk-Kubo et al., 2014; Bentzon-Tilia et al., 2015; Martinez-Perez et al., 2016; Pearl et al., 2018; Mills
342 et al., 2020). Besides, in Atlantic and Pacific Ocean areas when the diazotrophic community is dominated by unicellular
343 organisms, high N_2 fixation rates are mostly associated with a predominance of UCYN-A, and low rates with a
344 predominance of NCD (Turk-Kubo et al., 2014, Martinez-Perez et al., 2016; Moreira-Coello et al., 2017, Fonseca-Batista et
345 al., 2019; Tang et al., 2019).

346

347 **4.3 Intriguing Station 10**

348 The patchy distribution of the diazotrophic activity at Station 10 was related to an exceptionally high rate at the DCM (72.1
349 $nmol\ N\ L^{-1}\ d^{-1}$). High N_2 fixation rates have previously been observed locally: 2.4 $nmol\ N\ L^{-1}\ d^{-1}$ at the Strait of Gibraltar
350 (Rahav et al., 2013a), ~5 $nmol\ N\ L^{-1}\ d^{-1}$ in the Bay of Calvi (Rees et al., 2017), 17 $nmol\ N\ L^{-1}\ d^{-1}$ in the northwestern MS
351 (Garcia et al., 2006) and 129 $nmol\ N\ L^{-1}\ d^{-1}$ in the eastern MS (Rees et al., 2006). Station 10 was also hydrodynamically
352 "contrasted" compared to the other stations: it was located almost at the centre of an anticyclonic eddy (Guieu et al., 2020),
353 with the core waters (0-200 m) of Atlantic origin (colder, fresher). In such anticyclonic structures, enhanced exchange with
354 nutrients rich waters from below take place, combined with lateral mixing, could explain higher stocks of NO_3^- and DIP in
355 the euphotic layer (Table S1). Nevertheless, the anomaly of N_2 fixation at the DCM was neither associated with anomalies of
356 PP, BP nor NO_3^- and DIP concentrations. It only coincided with a minimum in DFe concentration (0.47 nM compared to 0.7
357 to 1.4 nM at the nearby depths, Bressac et al., 2021). Based on a range of Fe:C (from 7 to 177 $\mu mol: mol$) and associated C:N
358 ratios for diazotrophs (*Trichodesmium*, UCYN) from literature (Tuit et al., 2004; Berman-Frank et al., 2007; Jiang et al.,
359 2018), we found that 0.004 nM to 0.08 nM of DFe are required to sustain this N_2 fixation rate. Consequently, the minimum
360 in DFe concentration at 61m could not be explained solely by the diazotroph uptake.

361

362 Despite no correlation between N_2 fixation and the relative abundance of specific diazotrophs ($p > 0.05$) along the profile,
363 the huge heterogeneity in N_2 fixation rate was likely related to the patchy distribution of diazotrophs taxa. Indeed, patchiness
364 seems to be a common feature of unicellular diazotrophs (Robinart et al., 2014; Moreira-Coello et al., 2019). The
365 exceptionally high N_2 fixation rates coincided with the highest relative contributions of UCYN-A and more precisely
366 UCYN-A4. Exceptional N_2 fixation rates at Station 10, impacted by northeast Atlantic surface waters of subtropical origin
367 could thus be related to that incoming waters. Indeed, Fonseca-Batista et al. (2019) reported high N_2 fixation rates (45 and 65
368 $nmol\ N\ L^{-1}\ d^{-1}$ with euphotic N_2 fixation rates up to 1533 $\mu mol\ N\ m^{-2}\ d^{-1}$) associated with a predominance of UCYN-A in

369 subtropical Atlantic surface water mass along the Iberian Margin (~40° N-11° E). It should be noted that UCYN-A4 was
370 only detected at Station 10, and its relatively high contribution to the whole diazotrophic community in the euphotic layer
371 coincided with the highest stocks of P (and N) (Table S1). This could reflect higher nutrient requirement(s) of the UCYN-A4
372 and/or of its eukaryotic partner relative to other sublineages. Another intriguing feature was the high contribution (~86 %) of
373 UCYN-A in the mesopelagic zone (200 m). As UCYN-A lives in obligate symbiosis with haptophytes from which it
374 receives fixed carbon from photosynthesis (Thompson et al., 2012, 2014), this suggests that this contribution was probably
375 derived from sinking senescing prymnesiophyte-UCYN-A cells, and that the weak N₂ fixation rate at 200m depth is likely
376 only driven by γ -proteobacteria (*Pseudomonas*).

377

378 **4.4 Supply of bioavailable N from diazotrophic activity for fueling primary and heterotrophic bacterial production -** 379 **Relationship with potential controlling factors of N₂ fixation**

380 The relationship established between N₂ fixation, and PP and BP illustrated that in the studied area, N₂ fixation is promoted
381 by UCYN and NCD, and/or could indicate that all processes have the same (co)-limitation. Overall, N₂ fixation was a poor
382 contributor to PP (1.0 ± 0.3 %, Fig. S8), as previously shown in the MS (Bonnet et al., 2011; Yogeve et al., 2011; Rahav et al.
383 2013a) and BP (7 ± 1 %, Fig. S8) except at Station 10 where N₂ fixation could support up to 19 % of PP (Fig. S8) and supply
384 the entire bioavailable N requirements for heterotrophic prokaryotes (199 % of BP). As expected, our results suggest no
385 control of N₂ fixation by DFe and NO₃⁻, as previously shown through nutrient additions in microcosms (Rees et al., 2006;
386 Ridame et al., 2011, Rahav et al., 2016b). No correlation was observed between N₂ fixation and DIP which may highlight the
387 spatial variability of the controlling factor of diazotrophs as DIP was shown to control N₂ fixation in the western basin, but
388 not in the Ionian basin (Ridame et al., 2011). Moreover, DIP concentration does not reflect the rapid turnover of P in the
389 open MS and thus could be a poor indicator of DIP availability (Pulido-Villena et al., 2021).

390

391 **4.5 Diazotrophic activity and composition in response to dust addition under present climate conditions**

392 **General features** – In all experiments, simulated wet dust deposition under present climate conditions triggered a significant
393 (41 to 503 %) and rapid (24-48 h) stimulation of N₂ fixation relative to the controls. Despite this strong increase, N₂ fixation
394 rates remained low (< 0.7 nmol N L⁻¹ d⁻¹) as well as their contribution to PP (< 7 %) and BP (< 5 %) as observed *in situ*
395 (Sect.4.4). All of these results are consistent with those found after dust seeding in mesocosms in a coastal site in the
396 northwestern MS (Ridame et al., 2013) and in the open Cretan Sea (Rahav et al., 2016a).

397 **Temporal Changes in the composition of the diazotrophic community**- Dust addition under present climate conditions did
398 not impact the diazotrophic communities composition. At TYR and ION, the large increase in N₂ fixation recorded after dust
399 addition might be attributed to NCD (mainly γ -proteobacteria), as suggested by the positive correlation between N₂ fixation
400 and BP (Fig S4). At FAST, the community shifted from a large dominance of UCYN-A towards a dominance of NCD both
401 in the dust treatments and unamended controls due to the increase in a few fast growing γ -proteobacteria (mainly
402 *Pseudomonas*). This shift could be attributed to a bottle effect imposed by the tanks which can favor fast growing

403 heterotrophic bacteria (Sherr et al. 1999; Calvo-Diaz et al., 2011). Nevertheless, the increased N_2 fixation after dust seeding
404 at FAST cannot be explained by the shift in composition of the diazotrophic communities because the rates remained quite
405 stable in the controls all along the experiment. Rather, the abundances of diazotrophs have likely increased due to dust input,
406 and UCYN-A in association with prymnesiophytes could still be responsible for the majority of the enhanced N_2 fixation as
407 N_2 fixation correlated strongly with PP (Fig. S4).

408 **Variability of the N_2 fixation response among stations** - The highest stimulation of N_2 fixation to dust addition was
409 observed at TYR (mean $RC_D = 321$ %) then at ION (mean $RC_D = 161$ %) and finally at FAST (mean $RC_D = 21$ %) (Fig.7).
410 The differences in the intensity of the diazotrophic response were not related to differences in the initial nutrients stocks
411 (Table S1) and in the nutrients input from dust which was quite similar between experiments (Gazeau et al., 2021a). Briefly,
412 dust input led to a strong increase of $11.2 \pm 0.2 \mu M NO_3^-$ few hours after seeding in the three experiments, and the maximum
413 DIP release was slightly higher at FAST (31 nM) than at TYR and ION (23 ± 2 nM) (Gazeau et al., 2021a). As DFe
414 concentration before seeding was high (≥ 1.5 nM, Table 2), the bioavailability of Fe did not appear to drive the response of
415 N_2 fixation (Ridame et al., 2013). Also, we evidenced in this experiment that NO_3^- release from dust did not inhibit N_2
416 fixation rate driven by UCYN-A and NCD. This was expected for UCYN-A as it lacks NO_3^- assimilation pathways (Tripp et
417 al., 2010; Bombar et al., 2014).

418 N_2 fixation was initially more limited at TYR and ION (as evidenced by the lowest initial rates) compared to FAST, thereby
419 explaining the highest stimulation of N_2 fixation by dust seeding at these stations. Interestingly, the stimulation of N_2 fixation
420 was higher at TYR than at ION (Fig.7) while these stations presented the same initial rate supported by NCD. One major
421 difference is that PP was not enhanced by dust seeding at TYR while BP increased in both experiments (Gazeau et al.,
422 2021b) suggesting that NCD-supported N_2 fixation was not limited by organic carbon at this station. As N_2 fixation and BP
423 correlated strongly after the dust seeding (Fig. S4), it means that dust-derived DIP could relieve the ambient limitation of
424 both heterotrophic prokaryotes (BP was co-limited by NP, Van Wambeke et al., 2021) and NCD at TYR. This could explain
425 why DIP concentration in the D treatments became again similar to the controls at the end of this experiment (Gazeau et al.,
426 2021a). At ION characterized by the lowest initial DIP concentration, N_2 fixation and PP were likely DIP (co-)limited as
427 shown for BP (Van Wambeke et al., 2021). Consequently, diazotrophs as well as non diazotrophs (heterotrophic prokaryotes
428 and photoautotrophs) could all uptake the dust-derived DIP reducing then potentially the amount of DIP available for each
429 cell that could explain the lower stimulation of N_2 fixation relative to TYR.

430 At FAST, initially dominated by UCYN-A, N_2 fixation and PP correlated strongly after the dust seeding (Fig. S4c). This
431 indicated that dust could relieve either directly the ambient nutrient limitation of both N_2 fixation and PP (Fig.S9) or
432 indirectly through first the relief of the PP limitation of the UCYN-A photoautotroph hosts inducing an increase in the
433 production of organic carbon which could be used by UCYN-A to increase its N_2 -fixing activity. Nutrients from dust could
434 also first enhance the UCYN-A-supported N_2 fixation, which in turn could relieve the N limitation of the UCYN-A
435 photoautotrophic host, as the initial NO_3^-/DIP ratio indicates a potential N limitation of the PP (Table 2).

436

437 **4.6 Response to dust addition under future relative to present climate conditions**

438 **General features** -At TYR and FAST, N₂ fixation was more stimulated by dust input under future than present climate
439 conditions (mean RC_{G-TYR}= 478 % and mean RC_{G-FAST}= 54 %) whereas at ION the response was similar (Figs.7, S3). These
440 differences between future and present climate conditions were not related to the nutrients supplied from dust (Gazeau et al.,
441 2021a).

442 The purpose of our study was to study the combined effect of warming and acidification, but we can expect on the short time
443 scale of our experiments (< 3-4 days), that NCD and UCYN-A would not be directly affected by the changes in the CO₂
444 concentration as they do not fix CO₂ (Zehr et al., 2008). Indeed, no impact of acidification (or pCO₂ increase) on N₂ fixation
445 was detected when the diazotrophic communities were dominated by UCYN-A in the North and South Pacific (Law et al.,
446 2012; Böttjer et al. 2014). Nevertheless, the decrease in pH may indirectly impact UCYN-A through changes affecting its
447 autotrophic host.

448
449 **TYR and ION** –Under future climate conditions, the composition of the diazotrophic communities did not change after dust
450 input at TYR and ION relative to present conditions. At TYR, the highest N₂ fixation stimulation might be linked to the
451 increase in the NCD abundances and/or in their cell-specific N₂ fixation rates under future climate conditions. Unfortunately,
452 the impact of increased temperature and decreased pH on the cell-specific N₂ fixation rates of NCD is currently unknown.
453 However, some studies suggest a positive relationship between temperature and abundances of NCD: diazotrophic γ -
454 proteobacteria (γ -24774A11) gene copies correlated positively with temperature (from ~20 to 30° C) in surface waters of the
455 western South Pacific Ocean (Moisander et al., 2014), and Messer et al. (2015) suggested a temperature optima for these γ -
456 proteobacteria around 25-26° C in the Australian tropical waters. At ION, the similar stimulation of N₂ fixation by dust
457 under future climate conditions compared to present climate conditions could be explained by a greater mortality of
458 diazotrophs due to a higher grazing pressure and/or a higher viral activity. Indeed, higher bacterial mortality in the G
459 treatment that could be related to a higher grazing pressure has been observed (Dinasquet et al., 2021). Another explanation
460 is that in spite of the DIP supply from the dust, the DIP bioavailability, initially the lowest at ION, was not sufficient to allow
461 an additional N₂ fixation stimulation.

462 **FAST**- Some differences in the composition of the diazotrophic communities were observed between present and future
463 climate conditions at FAST after dust input: the contribution of NCD (mainly *Pseudomonas*) increased and that of UCYN-A
464 decreased. It must be noted that the duration of the experiment was longer at FAST (4 days) relative to TYR and ION (3
465 days) which could explain at least partly differences between stations. A direct response of increased temperature and/or
466 decreased pH can be considered on a very short time scale (12 hours) by comparing the results in the G treatment at T0 (+3°
467 C, -0.3 pH unit) with those in C and D treatments. The increased contribution of *Pseudomonas* in the G treatment at T0
468 (before dust addition) reveals a likely positive effect of temperature on the growth of this NCD as an increase in the top-
469 down control on the bacterioplankton was observed after dust seeding under future climate conditions (Dinasquet et al.,
470 2021). Interestingly, despite the decrease in the relative contribution of UCYN-A to the total diazotroph community after

471 dust addition, we observed contrasted responses within the UCYN-A group relative to present climate conditions: the
472 relative abundance of UCYN-A3 strongly decreased (4.6 % in G vs. 25.4 % in D) whereas the relative abundance of UCYN-
473 A2 was twice as high (7 % in G vs. 3.4 % in D). Notably, the relative contribution of UCYN-A1 did not appear to be
474 impacted during the dust addition experiment. These respective changes could be explained by the difference in the
475 temperature tolerance between UCYN-A2 and -A3. Temperature is one of the key drivers explaining the distribution of
476 UCYN-A which appeared to dominate in most of the temperate regions with temperature optima around ~20-24° C
477 (Langlois et al., 2008; Moisaner et al., 2010). However, the temperature optima for the different UCYN-A sublineages, in
478 particular for UCYN-A2 and -A3, are poorly known. Interestingly, Henke et al. (2018) observed that the absolute UCYN-A2
479 abundance was positively affected by increasing temperature, within a range of temperature from about 21 to 28° C which is
480 in agreement with our results although only relative abundances were measured in our study. Based on the strong positive
481 correlation between N₂ fixation and PP after dust addition (and no correlation between N₂ fixation and BP, Fig. S4), and
482 despite the decrease in the relative abundance of UCYN-A3, the increased stimulation of N₂ fixation under future climate
483 conditions could likely be sustained by the increase in the relative abundance of UCYN-A2 which is bigger than UCYN-A3
484 (Cornejo-Castillo et al., 2019) and could consequently have a higher cell-specific N₂ fixation rate.

485

486 **5. Conclusion**

487 In the MS, N₂ fixation is a minor pathway to supply new bioavailable N for sustaining both PP and BP but can locally
488 support up to 20 % of PP and provide all the N requirement for bacterial activity. UCYN-A might be supporting extremely
489 high rates of N₂ fixation (72 nmol.L⁻¹.d⁻¹) in the core of an eddy in the Algerian basin influenced by Atlantic waters. The
490 eastward decreasing longitudinal trend of N₂ fixation in the surface waters is likely related to the spatial variability of the
491 composition of the diazotrophic communities, as shown by the eastward increase in the relative abundance of NCD towards
492 more oligotrophic waters while we observed a westward increase in the relative abundance of UCYN-A. This could reflect
493 lower nutrients requirements for NCD relative to UCYN-A. Through the release of new nutrients, simulated wet dust
494 deposition under present and future climate conditions significantly stimulated N₂ fixation. The degree of stimulation
495 depended on the metabolic activity of the diazotrophs (degree of limitation) related to the composition of diazotrophic
496 communities, and on the ambient potential nutrient limitations of diazotrophs, including that of the UCYN-A
497 prymnesiophyte host. The strongest increase in N₂ fixation, not accompanied with a change in the composition of the
498 diazotrophic communities, was observed at the stations dominated by NCD (TYR, ION) where the nutrient limitation was
499 the strongest. Under projected future levels of temperature and pH, the dust effect is either exacerbated or unchanged.
500 Knowing that NCD and UCYN-A do not fix CO₂, we suggest that, on the time scale of our experiments (3-4 days), the
501 exacerbated response of N₂ fixation is likely the result of the warming (from about 21° C to 24° C) which may increase the
502 growth of NCD when nutrient availability allows it, and may alter the composition of UCYN-A community. However, to
503 date, the effect of acidification and temperature optima of the different UCYN-A sublineages are poorly known (or
504 unknown) as these UCYN-A remain uncultivated.

505 Future changes in climate, desertification and land use practices could induce an increase in dust deposition to the oceans
506 (Tegen et al., 2004; Moulin and Chiapello, 2006; Klingmüller et al., 2016). The predicted future increase in surface
507 temperature, and the resulting stronger stratification are expected to expand the surface of LNLC areas reinforcing
508 consequently the role of new nutrient supply from aeolian dust on the N₂ fixation and probably on the structure of the
509 diazotrophic communities.

510

511 **6. Data availability**

512 Guieu, C. et al. (2020). Biogeochemical dataset collected during the PEACETIME cruise. SEANOE.
513 <https://doi.org/10.17882/75747>.

514

515 **7. Author contributions**

516 FG and CG designed the dust seedings experiments. CR, JD, EB, MB, FVW, FG, VT, AT-S and CG participated to the
517 sampling and analysis. CR and EB performed DNA extraction; EB performed library preparation. CR, JD and SH analyzed
518 the data; CR wrote the manuscript with contributions from all authors.

519

520 **8. Competing interests**

521 The authors declare that they have no conflict of interest

522

523 **9. Special issue Statement**

524 This article is part of the special issue “Atmospheric deposition in the low-nutrient–low-chlorophyll (LNLC) ocean: effects
525 on marine life today and in the future (ACP/BG inter-journal SI)”. It is not associated with a conference.

526

527 **10. Financial support**

528 This study is a contribution to the PEACETIME project (<http://peacetime-project.org>), a joint initiative of the MERMEX and
529 ChArMEx components supported by CNRS-INSU, IFREMER, CEA, and Météo-France as part of the programme
530 MISTRALS coordinated by INSU. PEACETIME was endorsed as a process study by GEOTRACES. JD was funded by a
531 Marie Curie Actions-International Outgoing Fellowship (PIOF-GA-2013-629378). SH and LR were funded by grant 6108-
532 00013 from the Danish Council for independent research to LR.

533

534 **11. Acknowledgments**

535 The authors thank the captain and the crew of the RV Pourquoi Pas ? for their professionalism and their work at sea. We
536 warmly acknowledge our second ‘chieffe’ scientist Karine Desboeufs. We gratefully thank Eric Thiebaut and Pierre
537 Kostyrka for their precious advice with statistical tests. We also thank Kahina Djaoudi and Thibaut Wagener for their
538 assistance in sampling the tanks and TMC-rosette, Magloire Mandeng-Yogo and Fethiye Cetin for IRMS measurements at

539 the Alyses plate-form (SU, IRD). The DIC data used in this study were analyzed at the SNAPO-CO₂ service facility at
540 LOCEAN laboratory and supported by CNRS-INSU and OSU Ecce-Terra. We greatly appreciate the interest of the
541 reviewers and Christine Klaas, and thank them for their relevant comments and time spent reviewing our manuscript.

542

543 **12. References**

544 Aminot, A., and K  rouel, R.: Dosage automatique des nutriments dans les eaux marines, in: M  thodes d'analyses en milieu
545 marin, edited by: IFREMER, 188 pp, 2007.

546 Angel, R., Nepel, M., Panh  lzl, C., Schmidt, H., Herbold, C. W., Eichorst, S. A., and Woebken, D.: Evaluation of primers
547 targeting the diazotroph functional gene and development of NifMAP–A bioinformatics pipeline for analyzing nifH
548 amplicon data, *Front. Microbiol.*, 9, 703, <https://doi.org/10.3389/fmicb.2018.00703>, 2018.

549 Bar Zeev, E., Yogev, T., Man-Aharonovich, D., Kress, N., Herut, B., Beja, O., and Berman-Frank, I.: Seasonal dynamics of
550 the endosymbiotic, nitrogen-fixing cyanobacterium *Richelia intracellularis* in the Eastern Mediterranean Sea, *ISME J.*, 2,
551 911–92, <https://doi.org/10.1038/ismej.2008.56>, 2008.

552 Benavides, M., Bonnet, S., Hern  ndez, N., Mart  nez-P  rez, A. M., Nieto-Cid, M., and   lvarez-Salgado, X. A.: Basin-wide
553 N₂ fixation in the deep waters of the Mediterranean Sea, *Global Biogeochem. Cycles*, 30, 952–961,
554 <https://doi.org/10.1002/2015GB005326>, 2016.

555 Bentzon-Tilia, M., Traving, S. J., Mantikci, M., Knudsen-Leerbeck, H., Hansen, J. L. S., Markager, S., and Riemann, L.:
556 Significant N₂ fixation by heterotrophs, photoheterotrophs and heterocystous cyanobacteria in two temperate estuaries,
557 *ISME J.*, 9, <https://doi.org/10.1038/ismej.2014.119273>–85, 2015.

558 Berman-Frank, I.A., Quigg, A., Finkel, Z. V., Irwin, A.J., Haramaty, L.: Nitrogen-fixation strategies and Fe requirements in
559 cyanobacteria, *Limnol. Oceanogr.*, 52, 2260–2269, 2007.

560 Bigeard, E., Lopes Dos Santos, A., and Ribeiro, C.: nifH amplification for Illumina sequencing. protocols.io,
561 <https://dx.doi.org/10.17504/protocols.io.bkipkudn>, 2021.

562 Bonnet, S., and Guieu, C.: Atmospheric forcing on the annual in the Mediterranean Sea. A one year survey, *J. Geophys.*
563 *Res.*, 111, C09010, <https://doi.org/10.1029/2005JC003213>, 2006.

564 Bonnet, B., Grosso, O., and Moutin, T.: Planktonic dinitrogen fixation along a longitudinal gradient across the
565 Mediterranean Sea during the stratified period (BOUM cruise), *Biogeosciences*, 8, 2257–2267, <https://doi.org/10.5194/bg-8-2257-2011>, 2011.

567 Bosc, E., Bricaud, A., and Antoine, D.: Seasonal and interannual variability in algal biomass and primary production in the
568 Mediterranean Sea, as derived from 4 years of SeaWiFS observations, *Global Biogeochem. Cy.*, 18, GB1005,
569 <https://doi.org/10.1029/2003GB002034>, 2004.

570 Bolyen, E., Rideout, J. R., Dillon, M. R., Bokulich, N. A., Abnet, C. C., Al-Ghalith, G. A. et al.: Reproducible, interactive,
571 scalable and extensible microbiome data science using QIIME 2. *Nat. Biotechnol.*, 37, 852–857,
572 <https://doi.org/10.1038/s41587-019-0209-9>, 2019.

573 Bombar, D., Heller, P., Sanchez-Baracaldo, P., Carter, B. J., and Zehr, J.P.: Comparative genomics reveals surprising
574 divergence of two closely related strains of uncultivated UCYN-A cyanobacteria, *ISME J.*, 8, 2530–42,
575 <https://doi.org/10.1038/ismej.2014.167>, 2014.

576 B  ttjer, D., Karl, D. M., Letelier, R. M., Viviani, D. A., and Church, M. J.: Experimental assessment of diazotroph responses
577 to elevated seawater pCO₂ in the North Pacific Subtropical Gyre, *Global Biogeochem. Cycles*, 28, 601–616,
578 <https://doi.org/10.1002/2013GB004690>, 2014.

579 Bressac, M., Wagener, T., Leblond, N., Tovar-Sánchez, A., Ridame, C., Albani, S., Guasco, S., Dufour, A., Jacquet, S.,
580 Dulac, F., Desboeufs, K., and Guieu, C.: Subsurface iron accumulation and rapid aluminium removal in the Mediterranean
581 following African dust deposition, *Biogeosciences Discuss.*, <https://doi.org/10.5194/bg-2021-87>, in review, 2021.

582 Buchfink, B., Xie, C., and Huson, D. H.: Fast and sensitive protein alignment using DIAMOND, *Nat. methods*, 12, 1, 59-60,
583 <https://doi.org/10.1038/nmeth.3176>, 2015.

584 Callahan, B. J., Mc Murdie, P. J., Rosen, M. J., Han, A. W., Johnson, A. J. A., and Holmes, S.: DADA2: High-resolution
585 sample inference from Illumina amplicon data, *Nat. Methods*, 13, 581, <https://doi.org/10.1038/nmeth.3869>, 2016.

586 Clarke, K. R., and Warwick, P. E.: *Change in Marine Communities: An Approach to Statistical Analysis and Interpretation*,
587 Primer-E Ltd: Plymouth, UK, 2001.

588 Calvo-Díaz, A., Díaz-Pérez, L., Suárez, L. Á., Morán, X. A. G., Teira, E., and Marañón, E.: Decrease in the autotrophic-to-
589 heterotrophic biomass ratio of picoplankton in oligotrophic marine waters due to bottle enclosure. *Appl. Environ. Microbiol.*,
590 77, 5739–5746, <https://doi.org/10.1128/AEM.00066-11>, 2011.

591 Cornejo-Castillo, F. M., Munoz-Marin, M. D. C., Turk-Kubo, K. A., Royo-Llonch, M., Farnelid, H., Acinas, S.G., and Zehr,
592 J.P.: UCYN-A3, a newly characterized open ocean sublineage of the symbiotic N₂-fixing cyanobacterium candidate
593 *Atelocyanobacterium Thalassa*, *Environ. Microbiol.*, 21, 111–24, <https://doi.org/10.1111/1462-2920.14429>, 2019

594 Desboeufs, K. V., Losno, R., Colin, J.-L.: Factors influencing aerosol solubility during cloud processes. *Atmos. Environ.*, 35,
595 3529–3537, [https://doi.org/10.1016/S1352-2310\(00\)00472-6](https://doi.org/10.1016/S1352-2310(00)00472-6), 2001.

596 Desboeufs, K., Leblond, N., Wagener, T., Bon Nguyen, E., and Guieu, C.: Chemical fate and settling of mineral dust in
597 surface seawater after atmospheric deposition observed from dust seeding experiments in large mesocosms, *Biogeosciences*,
598 11, 5581-5594, <https://doi.org/10.5194/bg-11-5581-2014>, 2014.

599 Dinasquet, J., Bigeard, E., Gazeau, F., Azam, F., Guieu, C., Marañón, E., Ridame, C., Van Wambeke, F., Obernosterer, I.,
600 and Baudoux, A.-C.: Impact of dust addition on the microbial food web under present and future conditions of pH and
601 temperature, *Biogeosciences Discuss.*, <https://doi.org/10.5194/bg-2021-143>, in review, 2021.

602 D'Ortenzio, F., Iudicone, D., de Boyer Montegut, C., Testor, P., Antoine, D., Marullo, S., Santoleri, R., and Madec, G.:
603 Seasonal variability of the mixed layer depth in the Mediterranean Sea as derived from in situ profiles, *Geophys. Res. Lett.*,
604 32, <https://doi.org/10.1029/2005GL022463>, 2005.

605 D'Ortenzio, F., and Ribera d'Alcalà, M.: On the trophic regimes of the Mediterranean Sea: a satellite analysis,
606 *Biogeosciences*, 6, 139–148, <https://doi.org/10.5194/bg-6-139-2009>, 2009.

607 Eichner, M., Rost, B., and Kranz, S.: Diversity of ocean acidification effects on marine N₂ fixers, *J. Exp. Mar. Biol. Ecol.*,
608 457, 199-207, <https://doi.org/10.1016/j.jembe.2014.04.015>, 2014.

609 El Hourany, R., Abboud-Abi Saab, M., Faour, G., Mejia, C., Crépon, M., and Thiria, S.: Phytoplankton diversity in the
610 Mediterranean Sea from satellite data using self-organizing maps. *J. Geophys. Res-Oceans*, 124,
611 <https://doi.org/10.1029/2019JC015131>, 2019.

612 Farnelid, H., Turk-Kubo, K. A., del Carmen Muñoz-Marín, M., and Zehr, J. P.: New insights into the ecology of the globally
613 significant uncultured nitrogen-fixing symbiont UCYN-A, *Aquat. Microb. Ecol.*, 77, 3, 125-138,
614 <https://doi.org/10.3354/ame01794>, 2016.

615 Fonseca-Batista, D., Li, X., Riou, V., Michotey, V., Deman, F., Fripiat, F., Guasco, S., Brion, N., Lemaitre, N., Tonnard, M.,
616 Gallinari, M., Planquette, H., Planchon, F., Sarthou, G., Elskens, M., LaRoche, J., Chou, L., and Dehairs, F.: Evidence of
617 high N₂ fixation rates in the temperate northeast Atlantic, *Biogeosciences*, 16, 999–1017, [https://doi.org/10.5194/bg-16-999-](https://doi.org/10.5194/bg-16-999-2019)
618 2019, 2019.

619 Frank, I. E., Turk-Kubo, K. A., and Zehr, J. P.: Rapid annotation of nif H gene sequences using classification and regression
620 trees facilitates environmental functional gene analysis, *Env. microbiol. Rep.*, 8, 5, 905-916. [https://doi.org/10.1111/1758-](https://doi.org/10.1111/1758-2229.12455)
621 2229.12455, 2016.

- 622 Fu, F.-X., Mulholland, M. R., Garcia, N. S., Beck, A., Bernhardt, P. W., Warner, M. E., Sanudo-Wilhelmy, S. A., and
623 Hutchins, D. A.: Interactions between changing pCO₂, N₂ fixation, and Fe limitation in the marine unicellular
624 cyanobacterium *Crocospaera*, *Limnol. Oceanogr.*, 53, 2472–2484, <https://doi.org/10.4319/lo.2008.53.6.2472>, 2008.
- 625 Fu, F.-X., Yu, E., Garcia, N. S., Gale, Y., Luo, Y., Webb, E. A., and Hutchins, D.A.: Differing responses of marine N₂ fixers
626 to warming and consequences for future diazotroph community structure, *Aquat. Microb. Ecol.*, 72, 33–46,
627 <https://doi.org/10.3354/ame01683>, 2014.
- 628 Fukuda, R., Ogawa, H., Nagata, T., and Koike, I.: Direct determination of carbon and nitrogen contents of natural bacterial
629 assemblages in marine environments, *Applied and Environmental Microbiology*, 64(9), 3352–3358.
630 <https://doi.org/10.1128/aem.64.9.3352-3358.1998>, 1998.
- 631 Garcia, N., Raimbault, P., Gouze, E., and Sandroni, V.: Nitrogen fixation and primary production in Western Mediterranean,
632 *C. R. Biol.*, 329, 742–750, <https://doi.org/10.1016/j.crv.2006.06.006>, 2006.
- 633 Gazeau, F., Ridame, C., Van Wambeke, F., Alliouane, S., Stolpe, C., Irisson, J.-O., Marro, S., Dolan, J., Blasco, T., Grisoni,
634 J.-M., De Liège, G., Hélias-Nunige, S., Djaoudi, K., Pulido-Villena, E., Dinasquet, J., Obernosterer, I., Catala, P., Marie, B.,
635 and Guieu, C.: Impact of dust enrichment on Mediterranean plankton communities under present and future conditions of pH
636 and temperature: an overview, *Biogeosciences*, <https://doi.org/10.5194/bg-2020-202>, 2021a.
- 637 Gazeau, F., Van Wambeke, F., Marañón, E., Pérez-Lorenzo, M., Alliouane, S., Stolpe, C., Blasco, T., Leblond, N., Zäncker,
638 B., Engel, A., Marie, B., Dinasquet, J., and Guieu, C.: Impact of dust addition on the metabolism of Mediterranean plankton
639 communities and carbon export under present and future conditions of pH and temperature, *Biogeosciences*, 18, 5423–5446,
640 <https://doi.org/10.5194/bg-18-5423-2021>, 2021b.
- 641 Giorgi, F.: Climate change Hot-spots, *Geophys. Res. Lett.* 33, L08707, <https://doi.org/10.1029/2006GL025734>, 2006.
- 642 Guieu, C., Dulac, F., Desboeufs, K., Wagener, T., Pulido-Villena, E., Grisoni, J.-M., Louis, F., Ridame, C., Blain, S., Brunet,
643 C., Bon Nguyen, E., Tran, S., Labiadh, M., and Dominici, J.-M.: Large clean mesocosms and simulated dust deposition: a
644 new methodology to investigate responses of marine oligotrophic ecosystems to atmospheric inputs, *Biogeosciences*, 7,
645 2765–2784, <https://doi.org/10.5194/bg-7-2765-2010>, 2010.
- 646 Guieu, C., and Ridame, C.: Impact of atmospheric deposition on marine chemistry and biogeochemistry, in *Atmospheric
647 Chemistry in the Mediterranean Region: Comprehensive Diagnosis and Impacts*, edited by F. Dulac, S. Sauvage, and E.
648 Hamonou, Springer, Cham, Switzerland, 2020.
- 649 Guieu, C., D'Ortenzio, F., Dulac, F., Taillandier, V., Doglioli, A., Petrenko, A., Barrillon, S., Mallet, M., Nabat, P., and
650 Desboeufs, K.: Introduction: Process studies at the air–sea interface after atmospheric deposition in the Mediterranean Sea –
651 objectives and strategy of the PEACETIME oceanographic campaign (May–June 2017), *Biogeosciences*, 17, 5563–5585,
652 <https://doi.org/10.5194/bg-17-5563-2020>, 2020.
- 653 Hama, T., Miyazaki, T., Ogawa, Y., Iwakuma, T., Takahashi, M., Otsuki, A., and Ichimura, S.: Measurement of
654 photosynthetic production of a marine phytoplankton population using a stable ¹³C isotope, *Mar. biol.*, 73, 31–36,
655 <https://doi.org/10.1007/BF00396282>, 1983.
- 656 Henke, B. A., Turk-Kubo, K. A., Bonnet, S., and Zehr, J. P.: Distributions and Abundances of Sublineages of the N₂-Fixing
657 Cyanobacterium *Candidatus Atelocyanobacterium thalassa* (UCYN-A) in the New Caledonian Coral Lagoon, *Front.
658 Microbiol.*, 9, 554, <https://doi.org/10.3389/fmicb.2018.00554>, 2018.
- 659 Herut, B., T. Zohary, M. D. Krom, R. F. Mantoura, P. Pitta, S. Psarra, F. Rassoulzadegan, T. Tanaka, and Thingstad, T. F.:
660 Response of East Mediterranean surface water to Saharan dust: On-board microcosm experiment and field observations,
661 *Deep Sea Res., Part II*, 52, 3024–3040, <https://doi.org/10.1016/j.dsr2.2005.09.003>, 2005.
- 662 Herut, B., Rahav, E., Tsagaraki, T. M., Giannakourou, A., Tsiola, A., Psarra, S., Lagaria, A., Papageorgiou, N.,
663 Mihalopoulos, N., Theodosi, C. N., Violaki, K., Stathopoulou, E., Scoullou, M., Krom, M. D., Stockdale, A., Shi, Z.,
664 Berman-Frank, I., Meador, T. B., Tanaka, T., and Paraskevi, P.: The potential impact of Saharan dust and polluted aerosols

665 on microbial populations in the East Mediterranean Sea, an overview of a mesocosm experimental approach, *Front. Mar.*
666 *Sci.*, 3, 226, <https://doi.org/10.3389/fmars.2016.00226>, 2016.

667 Hutchins, D., Fu, F-X., Webb, E., Walworth, N., and Tagliabue, A.: Taxon-specific response of marine nitrogen fixers to
668 elevated carbon dioxide concentrations, *Nature Geosci* 6, 790–795, <https://doi.org/10.1038/ngeo1858>, 2013.

669 Ibello, V., Cantoni, C., Cozzi, S., and Civitarese, G.: First basin-wide experimental results on N₂ fixation in the open
670 Mediterranean Sea, *Geophys. Res. Lett.*, 37, L03608, <https://doi.org/10.1029/2009GL041635>, 2010.

671 Ignatiades, L., Gotsis-Skretas, O., Pagou, K., and Krasakopoulou, E.: Diversification of phytoplankton community structure
672 and related parameters along a large-scale longitudinal east-west transect of the Mediterranean Sea, *J. Plankton. Res.*, 31,
673 411–428, <https://doi.org/10.1093/plankt/fbn124>, 2009.

674 IPCC: IPCC Special Report on the Ocean and Cryosphere in a Changing Climate, edited by H. O. Pörtner, D. C. Roberts, V.
675 Masson-Delmotte, P. Zhai, M. Tignor, E. Poloczanska, K. Mintenbeck, A. Alegría, M. Nicolai, A. Okem, J. Petzold, B.
676 Rama, and N. M. Weyer., 2019.

677 Jiang, H. B., Fu, F-X., Rivero-Calle, S., Levine, N. M., Sañudo-Wilhelmy, S. A., Qu, P. P., Wang, X. W., Pinedo-Gonzalez,
678 P., Zhu, Z., and Hutchins, D.A.: Ocean warming alleviates iron limitation of marine nitrogen fixation, *Nature Clim. Change*,
679 8, 709–712, <https://doi.org/10.1038/s41558-018-0216-8>, 2018.

680 Klingmüller, K., Pozzer, A., Metzger, S., Stenchikov, G. L., and Lelieveld, J.: Aerosol optical depth trend over the Middle
681 East, *Atmos. Chem. Phys.*, 16, 5063–5073, <https://doi.org/10.5194/acp-16-5063-2016>, 2016.

682 Krom, M. D., Herut, B., and Mantoura, R. F. C.: Nutrient budget for the Eastern Mediterranean: Implications for phosphorus
683 limitation, *Limnol. Oceanogr.*, 49, 1582–1592, <https://doi.org/10.4319/lo.2004.49.5.1582>, 2004.

684 Krom, M. D., Emeis, K. C., and Van Cappellen, P.: Why is the Eastern Mediterranean phosphorus limited?, *Prog. Oceanogr.*,
685 85, 236–244, <https://doi.org/10.1016/j.pocean.2010.03.003>, 2010.

686 Langlois, R. J., Hümmer, D., and LaRoche, J.: Abundances and Distributions of the Dominant nifH Phylotypes in the
687 Northern Atlantic Ocean, *Appl. Env. Microbiol.*, 74, 6, 1922–31, <https://doi.org/10.1128/AEM.01720-07>, 2008.

688 Langlois, R. J., Mills, M. M., Ridame, C., Croot, P., and LaRoche, J.: Diazotrophic bacteria respond to Saharan dust
689 additions, *Mar. Ecol. Prog. Ser.*, 470, 1–14, <https://doi.org/10.3354/meps10109>, 2012.

690 Lazzari, P., Solidoro, C., Ibello, V., Salon, S., Teruzzi, A., Béranger, K., Colella, S., and Crise, A.: Seasonal and inter-annual
691 variability of plankton chlorophyll and primary production in the Mediterranean Sea: a modelling approach, *Biogeosciences*,
692 9, 217–233, <https://doi.org/10.5194/bg-9-217-2012>, 2012.

693 Law, C. S., Breitbarth, E., Hoffmann, L. J., McGraw, C. M. Langlois, R. J., LaRoche, J., Marriner, A., and Safi, K. A.: No
694 stimulation of nitrogen fixation by non-filamentous diazotrophs under elevated CO₂ in the South Pacific, *Glob. Change*
695 *Biol.*, 18, 3004–3014, <https://doi.org/10.1111/j.1365-2486.2012.02777.x>, 2012.

696 Lekunberri, I., Lefort, T., Romero, E., Vázquez-Domínguez, E., Romera-Castillo, C., Marrasé, C., Peters, F., Weinbauer, M.,
697 and Gasol, J. M.: Effects of a dust deposition event on coastal marine microbial abundance and activity, bacterial community
698 structure and ecosystem function, *J. Plankton Res.*, 32, 381–396, <https://doi.org/10.1093/plankt/fbp137>, 2010.

699 Le Moal, M., Collin, H., and Biegala, I.C.: Intriguing diversity among diazotrophic picoplankton along a Mediterranean
700 transect: a dominance of rhizobia, *Biogeosciences*, 8, 827-840, <https://doi.org/10.5194/bg-8-827-2011>, 2011 Louis et al., 2015.

701 Louis, J., Bressac, M., Pedrotti, M. L., and Guieu, C.: Dissolved inorganic nitrogen and phosphorus dynamics in abiotic
702 seawater following an artificial Saharan dust deposition, *Front. Mar. Sci.*, <https://doi.org/10.3389/fmars.2015.00027>, 2015.

703 Manca, B., Burca, M., Giorgetti, A., Coatanoan, C., Garcia, M.-J., and Iona, A.: Physical and biochemical averaged vertical
704 profiles in the Mediterranean regions: An important tool to trace the climatology of water masses and to validate incoming
705 data from operational oceanography, *J. Marine Syst.*, 48, 1–4, 83–116, <https://doi.org/10.1016/j.jmarsys.2003.11.025>, 2004.

706 Man-Aharonovich, D., Kress, N., Bar Zeev, E., Berman-Frank, I., and Beja, O.: Molecular ecology of nifH genes and
707 transcripts in the Eastern Mediterranean Sea, *Environ. Microbiol.*, 9, 9, 2354–2363, <https://doi.org/10.1111/j.1462->
708 2920.2007.01353.x, 2007.

709 Marañón, E., Van Wambeke, F., Uitz, J., Boss, E. S., Pérez-Lorenzo, M., Dinasquet, J., Haëntjens, N., Dimier, C., and
710 Taillandier, V.: Deep maxima of phytoplankton biomass, primary production and bacterial production in the Mediterranean
711 Sea during late spring, *Biogeosciences*, 18, 1749–1767, <https://doi.org/10.5194/bg-18-1749-2021>, 2021.

712 Martinez-Perez, C., Mohr, W., Loscher, C. R., Dekaezemacker, J., Littmann, S., Yilmaz, P., Lehnen, N., Fuchs, B. M.,
713 Lavik, G., Schmitz, R.A., LaRoche, J., and Kuypers, M. M.: The small unicellular diazotrophic symbiont, UCYN-A, is a key
714 player in the marine nitrogen cycle, *Nat. Microbiol.*, 1, 16163, <https://doi.org/10.1038/nmicrobiol.2016.163>, 2016.

715 Mas, J. L., Martin, J., Pham, M. K., Chamizo, E., Miquel, J-C., Osvath, I., Povinec, P. P., Eriksson, M., and Villa-Alfageme,
716 M.: Analysis of a major Aeolian dust input event and its impact on element fluxes and inventories at the DYFAMED site
717 (Northwestern Mediterranean), *Mar. Chem.*, 223, 103792, <https://doi.org/10.1016/j.marchem.2020.103792>, 2020.

718 Mermex Group, De Madron, X.D., Guieu, C., Sempere, R., Conan, P., Cossa, D., D'Ortenzio, F., Estournel, C., Gazeau, F.,
719 Rabouille, C., Stemann, L., Bonnet, S., Diaz, F., Koubbi, P., Radakovitch, O., Babin, M., Baklouti, M., Bancon-Montigny,
720 C., Belviso, S., Bensoussan, N., Bonsang, B., Bouloubassi, I., Brunet, C., Cadiou, J.F., Carlotti, F., Chami, M., Charmasson,
721 S., Charriere, B., Dachs, J., Doxaran, D., Dutay, J.C., Elbaz-Poulichet, F., Eleaume, M., Eyrolles, F., Fernandez, C., Fowler,
722 S., Francour, P., Gaertner, J.C., Galzin, R., Gasparini, S., Ghiglione, J.F., Gonzalez, J.L., Goyet, C., Guidi, L., Guizien, K.,
723 Heimburger, L.E., Jacquet, S.H.M., Jeffrey, W.H., Joux, F., Le Hir, P., Leblanc, K., Lefevre, D., Lejeusne, C., Leme, R.,
724 Loye-Pilot, M.D., Mallet, M., Mejanelle, L., Melin, F., Mellon, C., Merigot, B., Merle, P.L., Migon, C., Miller, W.L.,
725 Mortier, L., Mostajir, B., Mousseau, L., Moutin, T., Para, J., Perez, T., Petrenko, A., Poggiale, J.C., Prieur, L., Pujo-Pay, M.,
726 Pulido, V., Raimbault, P., Rees, A.P., Ridame, C., Rontani, J.F., Pino, D.R., Sicre, M.A., Taillandier, V., Tamburini, C.,
727 Tanaka, T., Taupier-Letage, I., Tedetti, M., Testor, P., Thebault, H., Thouvenin, B., Touratier, F., Tronczynski, J., Ulses, C.,
728 Van Wambeke, F., Vantrepotte, V., Vaz, S., and Verney, R.: Marine ecosystems' responses to climatic and anthropogenic
729 forcings in the Mediterranean, *Prog. Oceanogr.*, 91, 97-166, <https://doi.org/10.1016/j.pocean.2011.02.003>, 2011.

730 Messer, L. F., Doubell, M., Jeffries, T. C., Brown, M. V., and Seymour, J. R.: Prokaryotic and diazotrophic population
731 dynamics within a large oligotrophic inverse estuary, *Aquat. Microb. Ecol.*, 74, 1–15, <https://doi.org/10.3354/ame01726>,
732 2015.

733 Mills, M.M., Turk-Kubo, K.A., van Dijken, G.L., Henke, B.A., Harding, K., Wilson, S.T., Arrigo K.R., and Zehr, J.P.:
734 Unusual marine cyanobacteria/haptophyte symbiosis relies on N₂ fixation even in N-rich environments, *ISME J.*, 14, 2395–
735 2406, <https://doi.org/10.1038/s41396-020-0691-6>, 2020.

736 Moisander, P. H., Beinart, R. A., Hewson, I., White, A. E., Johnson, K. S., Carlson, C. A., Montoya, J. P., and Zehr, J. P.:
737 Unicellular cyanobacterial distributions broaden the oceanic N₂ fixation domain, *Science*, 327, 5972, 1512–1514,
738 <https://doi.org/10.1126/science.1185468>, 2010.

739 Moisander, P. H., Serros, T., Paerl, R. W., Beinart, R. A., Zehr, J. P.: Gammaproteobacterial diazotrophs and nifH gene
740 expression in surface waters of the South Pacific Ocean, *ISME J.*, 8, 10, 1962–73, <https://doi.org/10.1038/ismej.2014.49>,
741 2014.

742 Montoya, J. P., Voss, M., Kahler, P., and Capone, D. G.: A simple, high-precision, high-sensitivity tracer assay for N₂
743 fixation, *App. Environ. Microbiol.*, 62, 3, 986-993, <https://doi.org/10.1128/AEM.62.3.986-993.1996>, 1996.

744 Mohr, W., Grosskopf, T., Wallace, D. R. W., and LaRoche, J.: Methodological underestimation of oceanic nitrogen fixation
745 rates, *PLoS One*, 5, 1–7, <https://doi.org/10.1371/journal.pone.0012583>, 2010.

746 Moreira-Coello, V., Mouriño-Carballido, B., Marañón, E., Fernández-Carrera, A., Bode, A., and Varela, M. M.: Biological
747 N₂ Fixation in the Upwelling Region off NW Iberia: Magnitude, Relevance, and Players, *Front. Mar. Sci.*, 4, 303,
748 <https://doi.org/10.3389/fmars.2017.00303>, 2017.

749 Moreira-Coello, V., Mouriño-Carballido, B., Marañón, E., Fernández-Carrera, A. Bode, A., Sintés, E., Zehr, J.P., Turk-
750 Kubo, K., and Varela, M.M.: Temporal variability of diazotroph community composition in the upwelling region off NW
751 Iberia, *Sci. Rep.*, 9, 3737, <https://doi.org/10.1038/s41598-019-39586-4>, 2019.

752 Moulin, C., and Chiapello, I.: Impact of human-induced desertification on the intensification of Sahel dust emission and
753 export over the last decades, *Geophys. Res. Lett.*, 33, <https://doi.org/10.1029/2006GL025923>, 2006.

754 Moynihan, M.A.: nifHdada2 GitHub repository, Zenodo, <http://doi.org/10.5281/zenodo.3958370>, 2020

755 Paerl, R. W., Hansen, T. N. G., Henriksen, N. S. E., Olesen, A. K., and Riemann, L.: N-fixation and related O₂ constraints
756 on model marine diazotroph *Pseudomonas stutzeri* BAL361, *Aquatic Microbial Ecology*, 81, 125–136,
757 <https://doi.org/10.3354/ame01867>, 2018.

758 Pierella Karlusich, J.J., Pelletier, E., Lombard, F., Carsique, M., Dvorak, E., Colin, S., Picheral, M., Cornejo-Castillo, F. M.,
759 Acinas, S. G., Pepperkok, R., Karsenti, E., de Vargas, C., Wincker, P., Bowler, C., and Foster, R. A.: Global distribution
760 patterns of marine nitrogen-fixers by imaging and molecular methods, *Nat. Commun.*, 12, 4160,
761 <https://doi.org/10.1038/s41467-021-24299-y>, 2021.

762 Pulido-Villena, E., Wagener, T., and Guieu, C.: Bacterial response to dust pulses in the western Mediterranean: Implications
763 for carbon cycling in the oligotrophic ocean, *Global Biogeochem. Cycles*, 22, GB1020,
764 <https://doi.org/10.1029/2007GB003091>, 2008.

765 Pulido-Villena, E., Rérolle, V., and Guieu, C.: Transient fertilizing effect of dust in P-deficient LNLC surface ocean,
766 *Geophys. Res. Lett.*, 37, L01603, <https://doi.org/10.1029/2009GL041415>, 2010.

767 Pulido-Villena, E., Baudoux, A. C., Obernosterer, I., Landa, M., Caparros, J., Catala, P., Georges, C., Harmand, J., and
768 Guieu, C.: Microbial food web dynamics in response to a Saharan dust event: results from a mesocosm study in the
769 oligotrophic Mediterranean Sea, *Biogeosciences*, 11, 5607-5619, [10.5194/bg-11-5607-2014](https://doi.org/10.5194/bg-11-5607-2014), 2014.

770 Pulido-Villena, E., Desboeufs, K., Djaoudi, K., Van Wambeke, F., Barrillon, S., Doglioli, A., Petrenko, A., Taillandier, V.,
771 Fu, F., Gaillard, T., Guasco, S., Nunige, S., Triquet, S., and Guieu, C.: Phosphorus cycling in the upper waters of the
772 Mediterranean Sea (Peacetime cruise): relative contribution of external and internal sources, *Biogeosciences*, 18, 5871–5889,
773 <https://doi.org/10.5194/bg-18-5871-2021>, 2021.

774 Rahav, E., Herut, B., Levi, A., Mulholland, M. R., and Berman-Frank, I.: Springtime contribution of dinitrogen fixation to
775 primary production across the Mediterranean Sea, *Ocean Sci.*, 9, 489–498, <https://doi.org/10.5194/os-9-489-2013>, 2013a.

776 Rahav, E., Bar-Zeev, E., Ohayon, S., Elifantz, H., Belkin, N., Herut, B., Mulholland, M. R., and Berman-Frank, I.:
777 Dinitrogen fixation in aphotic oxygenated marine environments, *Front. Microbiol.*, 4, 227,
778 <https://doi.org/10.3389/fmicb.2013.00227>, 2013b.

779 Rahav, E., Shun-Yan, C., Cui, G., Liu, H., Tsagaraki, T. M., Giannakourou, A., Tsiola, A., Psarra, S., Lagaria, A.,
780 Mulholland, M. R., Stathopoulou, E., Paraskevi, P., Herut, B., and Berman-Frank, I.: Evaluating the impact of atmospheric
781 depositions on springtime dinitrogen fixation in the Cretan Sea (eastern Mediterranean)—A mesocosm approach, *Front.*
782 *Mar. Sci.*, 3, 180, <https://doi.org/10.3389/fmars.2016.00180>, 2016a.

783 Rahav, E., Giannetto, J.M., and Bar-Zeev, E.: Contribution of mono and polysaccharides to heterotrophic N₂ fixation at the
784 eastern Mediterranean coastline, *Sci. Rep.*, 6, 27858, <https://doi.org/10.1038/srep27858>, 2016b.

785 Rees, A. P., Law, C. S., and Woodward, E. M. S.: High rates of nitrogen fixation during an in-situ phosphate release
786 experiment in the Eastern Mediterranean Sea, *Geophys. Res. Lett.*, 33, L10607, <https://doi.org/10.1029/2006GL025791>, 2006.

787 Rees, A. P., Turk-Kubo, K. A., Al-Moosawi, L., Alliouane, S., Gazeau, F., Hogan, M. E. and Zehr, J.P.: Ocean acidification
788 impacts on nitrogen fixation in the coastal western Mediterranean Sea, *Estuarine, Coastal and Shelf Science*, 186, Part A, 45-
789 57, <https://doi.org/10.1016/j.ecss.2016.01.020>, 2017.

790 Ridame, C., Le Moal, M., Guieu, C., Ternon, E., Biegala, I. C., L'Helguen, S., and Pujo-Pay M.: Nutrient control of N₂
791 fixation in the oligotrophic Mediterranean Sea and the impact of Saharan dust events, *Biogeosciences*, 8, 2773-
792 2783, <https://doi.org/10.5194/bg-8-2773-2011>, 2011.

793 Ridame, C., Guieu, C., and L'Helguen, S.: Strong stimulation of N₂ fixation in oligotrophic Mediterranean Sea: results from
794 dust addition in large in situ mesocosms, *Biogeosciences*, 10, 7333-7346, <https://doi.org/10.5194/bg-10-7333-2013>, 2013.

795 Ridame, C., Dekaezemacker, J., Guieu, C., Bonnet, S., L'Helguen, S., and Malien, F.: Contrasted Saharan dust events in
796 LNLC environments: impact on nutrient dynamics and primary production, *Biogeosciences*, 11, 4783-
797 4800, <https://doi.org/10.5194/bg-11-4783-2014>, 2014.

798 Robidart, J., Church, M., Ryan, J., Ascani, F., Wilson, S. T., Bombar, D., Marin III, R., Richards, K. J., Karl, D. M., Scholin,
799 C. A., and Zehr, J.P.: Ecogenomic sensor reveals controls on N₂-fixing microorganisms in the North Pacific Ocean, *ISME J.*,
800 8, 1175–1185, <https://doi.org/10.1038/ismej.2013.244>, 2014.

801 Roy-Barman, M., Foliot, L., Douville, E., Leblond, N., Gazeau, F., Bressac, M., Wagener, T., Ridame, C., Desboeufs, K.,
802 and Guieu, C.: Contrasted release of insoluble elements (Fe, Al, rare earth elements, Th, Pa) after dust deposition in
803 seawater: a tank experiment approach, *Biogeosciences*, 18, 2663–2678, <https://doi.org/10.5194/bg-18-2663-2021>, 2021.

804 Sherr, E. B., Sherr, B. F., and Sigmon, C. T.: Activity of marine bacteria under incubated and in situ conditions, *Aquatic*
805 *Microbial Ecol.*, 20, 213-223, 1999.

806 Siokou-Frangou, I., Christaki, U., Mazzocchi, M. G., Montresor, M., Ribera d'Alcalá, M., Vaqué, D., and Zingone, A.:
807 Plankton in the open Mediterranean Sea: A review, *Biogeosciences*, 7, 5, 1543–1586, [https://doi.org/10.5194/bg-7-1543-](https://doi.org/10.5194/bg-7-1543-2010)
808 2010, 2010.

809 Smith, D. C. and Azam, F.: A simple, economical method for measuring bacterial protein synthesis rates in sea water using
810 3H-Leucine, *Mar. Microb. Food Webs*, 6, 107-114, 1992.

811 Somot, S., Sevault, F., Deque, M., and Crepon, M.: 21st century climate change scenario for the Mediterranean using a
812 coupled atmosphere – ocean regional climate model, *Global Planet Change*, 63, 112–126,
813 <https://doi.org/10.1016/j.gloplacha.2007.10.003>, 2008.

814 Tang, W., Wang, S., Fonseca-Batista, D., Dehairs, F., Gifford, S., Gonzalez, A. G., Gallinari, M., Planquette, H., Sarthou, G.,
815 and Cassar, N.: Revisiting the distribution of oceanic N₂ fixation and estimating diazotrophic contribution to marine
816 production, *Nat. Commun.*, 10, 831, <https://doi.org/10.1038/s41467-019-08640-0>, 2019.

817 Tegen, I., Werner, M., Harrison, S. P., and Kohfeld, K. E.: Relative importance of climate and land use in determining
818 present and future global soil dust emissions, *Geophys. Res. Lett.*, 31, L05105, <https://doi.org/10.1029/2003GL019216>,
819 2004.

820 Ternon E., Guieu, C., Ridame, C., L'Helguen, S., and Catala, P.: Longitudinal variability of the biogeochemical role of
821 Mediterranean aerosols in the Mediterranean Sea, *Biogeosciences*, 8, 1067-1080, <https://doi.org/10.5194/bg-8-1067-2011>,
822 2011.

823 Thompson, A. W., Foster, R. A., Krupke, A., Carter, B. J., Musat, N., Vaultot, D., Kuypers, M. M. M., Zehr, J. P.:
824 Unicellular cyanobacterium symbiotic with a single-celled eukaryotic alga, *Science*, 337, 1546–50.
825 <https://doi.org/10.1126/science.1222700>, 2012.

826 Thompson, A., Carter, B. J., Turk-Kubo, K., Malfatti, F., Azam, F., and Zehr, J. P.: Genetic diversity of the unicellular
827 nitrogen-fixing cyanobacteria UCYN-A and its prymnesiophyte host, *Environ. Microbiol.*, 16, 3238–49,
828 <https://doi.org/10.1111/1462-2920.12490>, 2014.

829 Tovar-Sánchez, A., Rodríguez-Romero, A., Engel, A., Zäncker, B., Fu, F., Marañón, E., Pérez-Lorenzo, M., Bressac, M.,
830 Wagener, T., Triquet, S., Siour, G., Desboeufs, K., and Guieu, C.: Characterizing the surface microlayer in the
831 Mediterranean Sea: trace metal concentrations and microbial plankton abundance, *Biogeosciences*, 17, 2349–2364,
832 <https://doi.org/10.5194/bg-17-2349-2020>, 2020.

833 Tripp, H. J., Bench, S. R., Turk, K. A., Foster, R. A., Desany, B. A., Niazi, F., Affourtit, J. P., and Zehr, J. P.: Metabolic
834 streamlining in an open-ocean nitrogen-fixing cyanobacterium, *Nature*, 464, 90–94, <https://doi.org/10.1038/nature08786>,
835 2010.

836 Tuit, C., Waterbury, J., Ravizza, G.: Diel variation of molybdenum and iron in marine diazotrophic cyanobacteria, *Limnol.*
837 *Oceanogr.*, 49, 978–990, doi:10.4319/lo.2004.49.4.0978, 2004

838 Turk-Kubo, K. A., Farnelid, H. M., Shilova, I. N., Henke, B., and Zehr, J. P.: Distinct ecological niches of marine symbiotic
839 N₂-fixing cyanobacterium *Candidatus Atelocyanobacterium thalassa* sublineages, *J. phycol.*, 53, 2, 451–461,
840 <https://doi.org/10.1111/jpy.12505>, 2017.

841 Turk-Kubo, K. A., Karamchandani, M., Capone, D. G., and Zehr, J.P.: The paradox of marine heterotrophic nitrogen
842 fixation: abundances of heterotrophic diazotrophs do not account for nitrogen fixation rates in the Eastern Tropical South
843 Pacific, *Environmental Microbiology*, 16, 10, 3095–3114, <https://doi.org/doi:10.1111/1462-2920.12346>, 2014.

844 Van Wambeke, F., Taillandier, V., Deboeufs, K., Pulido-Villena, E., Dinasquet, J., Engel, A., Marañón, E., Ridame, C., and
845 Guieu, C.: Influence of atmospheric deposition on biogeochemical cycles in an oligotrophic ocean system, *Biogeosciences*,
846 18, 5699–5717, <https://doi.org/10.5194/bg-18-5699-2021>, 2021.

847 Wang, Q., Quensen, J. F., Fish, J. A., Lee, T. K., Sun, Y., Tiedje, J. M., and Cole, J. R.: Ecological patterns of nifH genes in
848 four terrestrial climatic zones explored with targeted metagenomics using FrameBot, a new informatics tool, *MBio*, 4, 5,
849 <https://doi.org/10.1128/mBio.00592-13>, 2013.

850 Webb, E. A., Ehrenreich, I. A., Brown, S. L., Valois, F. W., and Waterbury, J. B.: Phenotypic and genotypic characterization
851 of multiple strains of the diazotrophic cyanobacterium, *Crocospaera watsonii*, isolated from the open ocean, *Env.*
852 *Microbiol.*, 11, 2, 338–348, <https://doi.org/10.1111/j.1462-2920.2008.01771.x>, 2008.

853 Yogeve, T., Rahav, E., Bar-Zeev, E., Man-Aharonovich, D., Stambler, N., Kress, N., Béjà, O., Mulholland, M. R., Herut, B.,
854 and Berman-Frank, I.: Is dinitrogen fixation significant in the Levantine Basin, East Mediterranean Sea?, *Environ.*
855 *Microbiol.*, 13, 4, 854–871, <https://doi.org/10.1111/j.1462-2920.2010.02402.x>, 2011.

856 Zehr, J. P., Mellon, M. T., and Zani, S.: New nitrogen fixing microorganisms detected in oligotrophic oceans by the
857 amplification of nitrogenase (nifH) genes, *Appl. Environ. Microbiol.*, 64, 3444–50, [https://doi.org/10.1128/AEM.64.9.3444-](https://doi.org/10.1128/AEM.64.9.3444-3450.1998)
858 [3450.1998](https://doi.org/10.1128/AEM.64.9.3444-3450.1998), 1998.

859 Zehr, J. P., Bench, S. R., Carter, B. J., Hewson, I. and Niazi, F.: Globally Distributed Uncultivated Oceanic N₂-Fixing
860 Cyanobacteria Lack Oxygenic Photosystem II, *Science*, 322, 1110, <https://doi.org/10.1126/science.1165340>, 2008.

861

862

863

864

865

866

867

868

869

870

871

872 **Table 1:** Integrated N₂ fixation over the surface mixed layer (SML, from surface to the mixed layer depth), from the surface
873 to the base of the euphotic layer (1% PAR depth), over the aphotic layer (1%PAR depth to 1000 m), and from surface to
874 1000 m at all the sampled stations. Contribution (in %) of SML integrated N₂ fixation to euphotic layer integrated N₂
875 fixation, and contribution of euphotic layer integrated N₂ fixation to total (0-1000 m) integrated N₂ fixation.
876

	N ₂ Fix _{SML}	N ₂ Fix _{euphotic}	N ₂ Fix _{aphotic}	N ₂ Fix _{0-1000m}	N ₂ Fix _{SML} /N ₂ Fix _{euphotic}	N ₂ Fix _{euphotic} /N ₂ Fix 0-1000m
	μmolN m ⁻² d ⁻¹	μmolN m ⁻² d ⁻¹	μmolN m ⁻² d ⁻¹	μmolN m ⁻² d ⁻¹	%	%
ST01	14.6	42.6	56.5	99.1	34	43
ST02	10.7	36.0	16.0	51.9	30	69
ST03	7.8	58.3	18.1	76.4	13	76
ST04	10.8	46.6	38.5	85.1	23	55
ST05	4.9	46.3	36.1	82.4	10	56
TYR	4.2	38.6	53.0	91.6	11	42
ST06	9.1	34.9	29.8	64.7	26	54
ST07	10.5	43.5	55.4	98.8	24	44
ION	6.2	40.6	56.5	97.1	15	42
ST08	4.3	27.0	12.3	39.3	16	69
ST09	3.4	50.2	43.3	93.5	7	54
FAST	5.9	58.2	35.7	93.8	10	62
ST10	13.7	1908	63.7	1972	1	97
Mean ± std (ST10 excluded)	7.7±3.5	44±9	38±16	81±20	18%±9%	55%±12%
Mean ± std (all stations)	8.2±3.7	187±517	40±17	227±525	17%±10%	59%±16%

877

878

879

880

881

882

883

884 **Table 2:** Initial physico-chemical and biological properties of surface seawater before the perturbation in the dust seeding
885 experiments at TYR, ION and FAST (average at T0 in C and D treatments, n=4 or data at T-12h in the pumped surface
886 waters, n=1). The relative abundances of diazotrophic cyanobacteria and NCD (non-cyanobacterial diazotroph) are given as
887 proportion of total *nifH* sequence reads. DIP: dissolved inorganic phosphorus, DFe: dissolved iron. The C:N ratio
888 corresponds to the ratio in the organic particulate matter from IRMS measurements (> 0.7µm). Means that did not differ
889 significantly between the experiments (p>0.05) are labeled with the same letter (in parenthesis).
890

	TYR	ION	FAST
Day of sampling	05/17/2017	05/25/2017	06/02/2017
Temperature (° C)*	20.6	21.2	21.5
Salinity*	37.96	39.02	37.07
¹³ C-Primary production, mg C m ⁻³ d ⁻¹	1.23±0.64 (A)	2.53±0.40 (B)	2.82±0.55 (B)
N ₂ fixation nmol N L ⁻¹ d ⁻¹	0.19±0.03 (A)	0.21±0.05 (A)	0.51±0.04 (B)
Relative abundance of diazotrophic cyanobacteria (%)	4.7±3.8 (A)	6.2±6.5 (A)	91.4±6.0 (B)
Relative abundance of NCD (%)	95.3±3.9 (A)	93.8±6.5 (A)	8.6±6.0 (B)
Heterotrophic bacterial production ng C. L ⁻¹ h ⁻¹	26.6 ± 7.0 (AB)	25.9 ± 0.9 (A)	36.3 ± 1.2 (B)
C:N (mol/mol)	9.6±0.8 (A)	10.2±0.8 (A)	9.1±0.5 (A)
DIP, nM*	17	7	13
NO ₃ ⁻ , nM*	14	18	59
NO ₃ ⁻ /DIP, mol/mol	0.8	2.6	4.5
DFe, nM [§]	1.5±0.1 (A)	2.6±0.2 (B)	1.8±0.2 (A)

891 * from Gazeau et al., 2021a

892 § from Roy-Barman et al., 2021

893

894

895

896

897

898

899

900

901

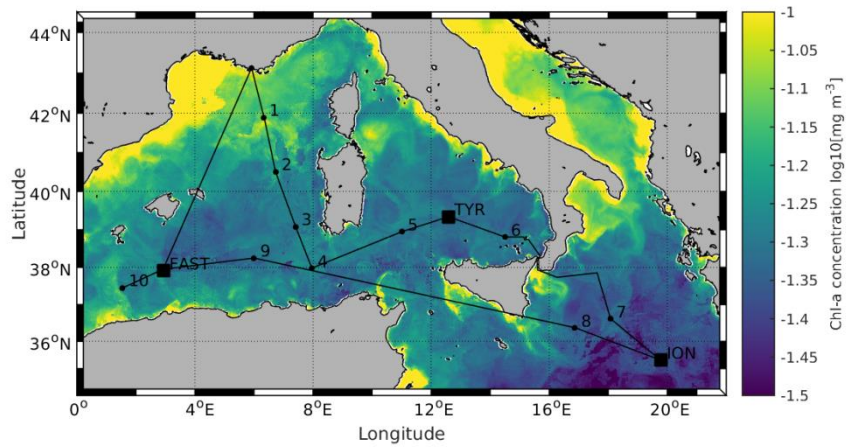
902

903

904 Figure 1: Locations of the ten short (ST1 to ST10) and three long stations (TYR, ION and FAST). Stations 1 and 2 were
905 located in the Provencal basin; Stations 5, 6, and TYR, in the Tyrrhenian Sea; Stations 7, 8, and ION in the Ionian Sea; and
906 Stations 3, 4, 9, 10 and FAST in the Algerian basin. Satellite-derived surface chlorophyll-a concentration (mg m^{-3}) averaged
907 over the entire duration of the PEACETIME cruise (Courtesy of Louise Rousselet)

908

909



910

911

912

913

914

915

916

917

918

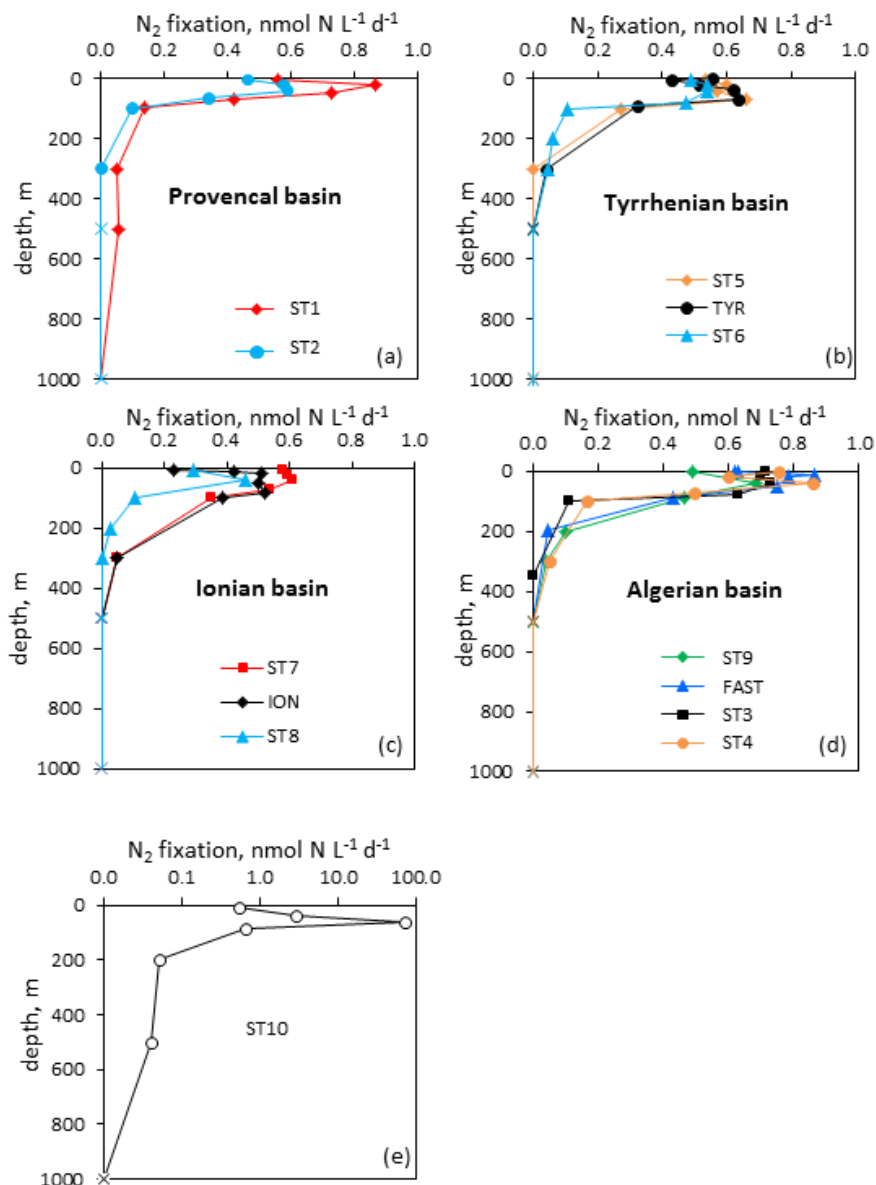
919

920

921

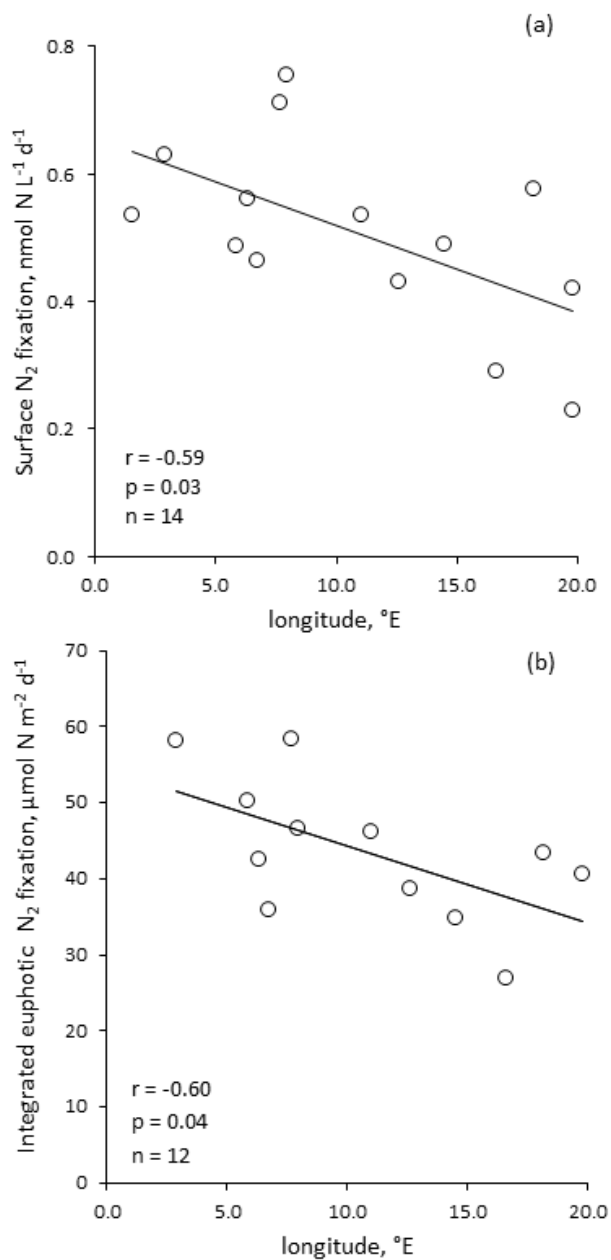
922

923 Figure 2: Vertical distribution of N_2 fixation (in $\text{nmol N L}^{-1} \text{d}^{-1}$) in the Provencal (a), Tyrrhenian (b) Ionian (c) and Algerian (d) basins and at Station 10 (e). N_2 fixation rates at Station 10 are plotted in log scale because of the high fluxes. Rates under
 924 detection limit ($<0.04 \text{ nmol N L}^{-1} \text{d}^{-1}$) are symbolized by crosses.
 925
 926



927
 928
 929

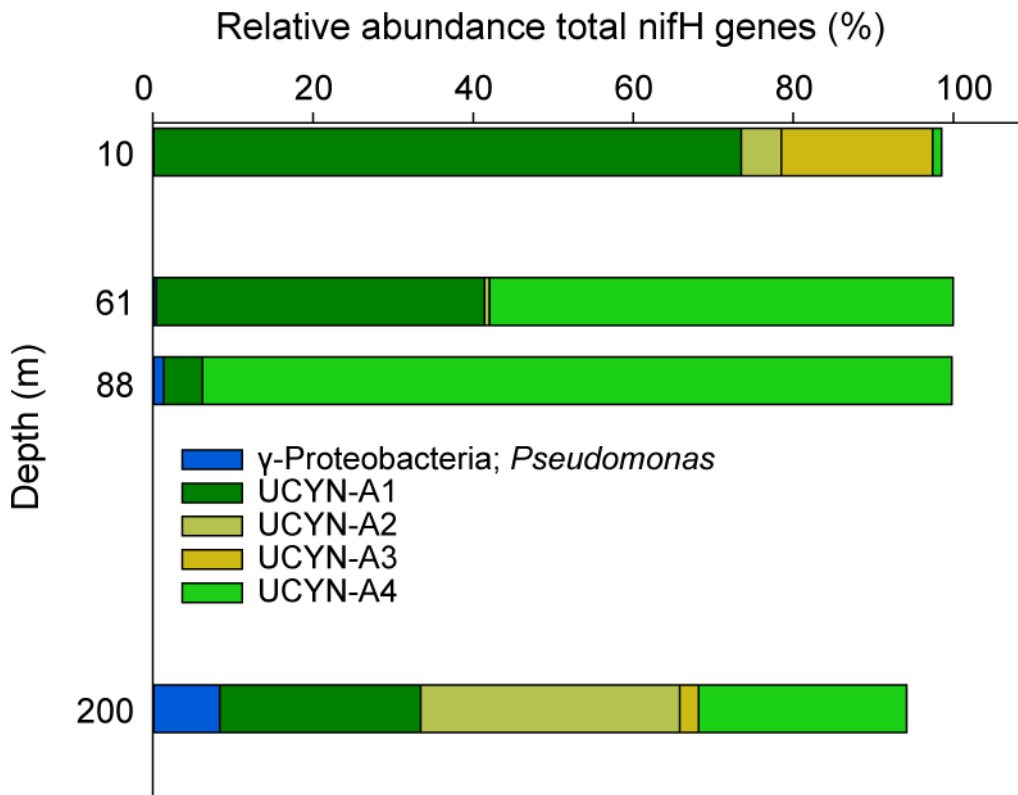
930 Figure 3: Volumetric surface (~5m) (a) and integrated N₂ fixation from surface to euphotic layer depth (b) along the
931 longitudinal PEACETIME transect (Station 10 was excluded). Integrated N₂ fixation rate from Station 10 was excluded from
932 statistical analysis
933



934

935 Figure 4: Vertical distribution of the 20 most abundant nifH-ASVs at Station 10, collapsed into major taxonomic groups.

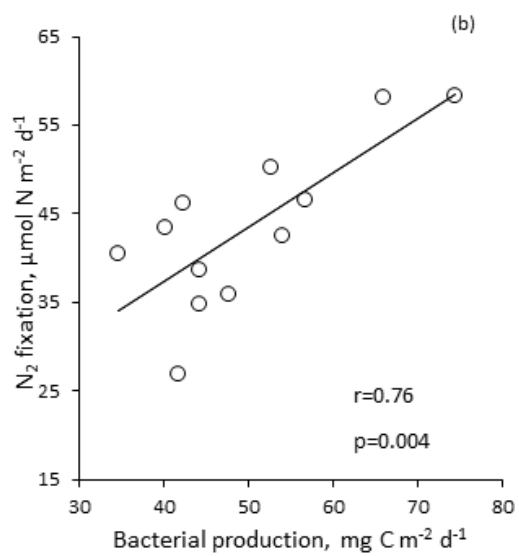
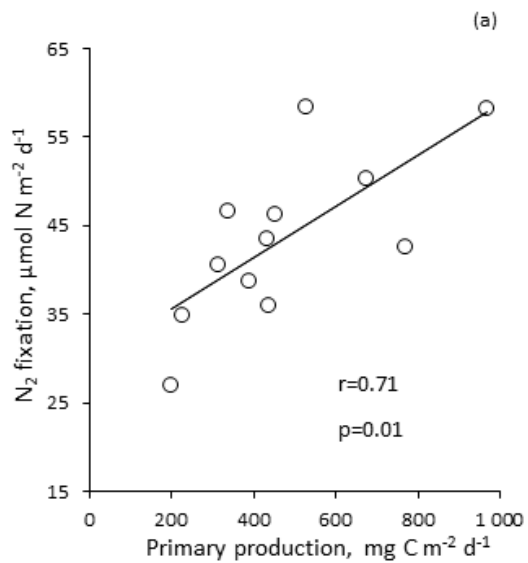
936
937
938
939
940



941
942
943
944
945
946
947
948

949 Figure 5: N_2 fixation rate integrated over the euphotic layer versus ^{13}C -primary production (a) and bacterial production (b);
950 data at Station 10 were removed.

951



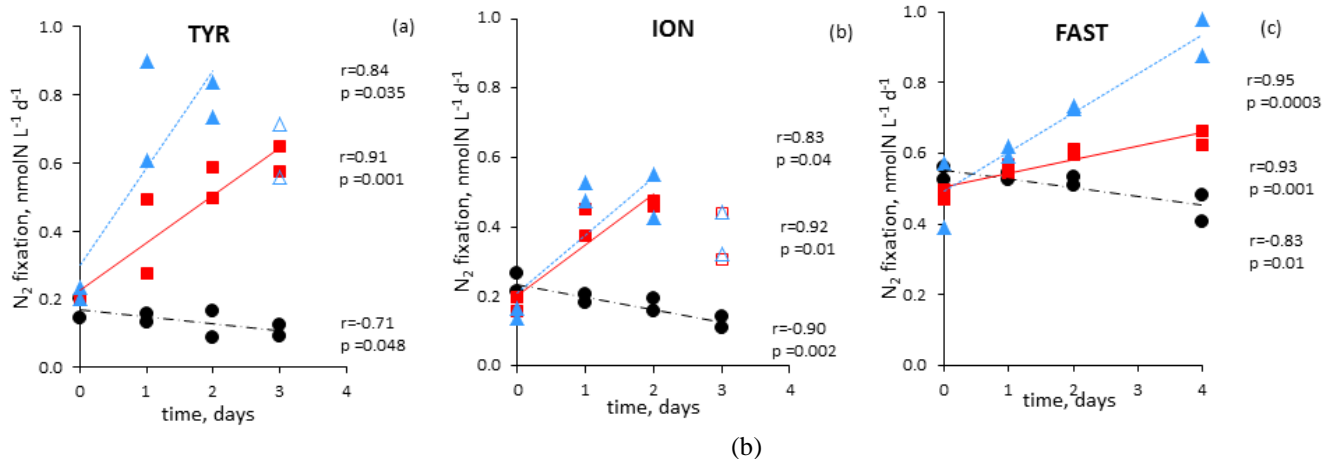
952

953

954

955

956 Figure 6: N₂ fixation rate in nmol N L⁻¹ d⁻¹ during the dust seeding experiments performed at the stations TYR (a), ION (b)
 957 and FAST (c) in the replicated controls (black dot), dust treatments under present climate conditions (red square, D
 958 treatment) and dust treatments under future climate conditions (green triangle, G treatment). Open symbols were not
 959 included in the linear regression

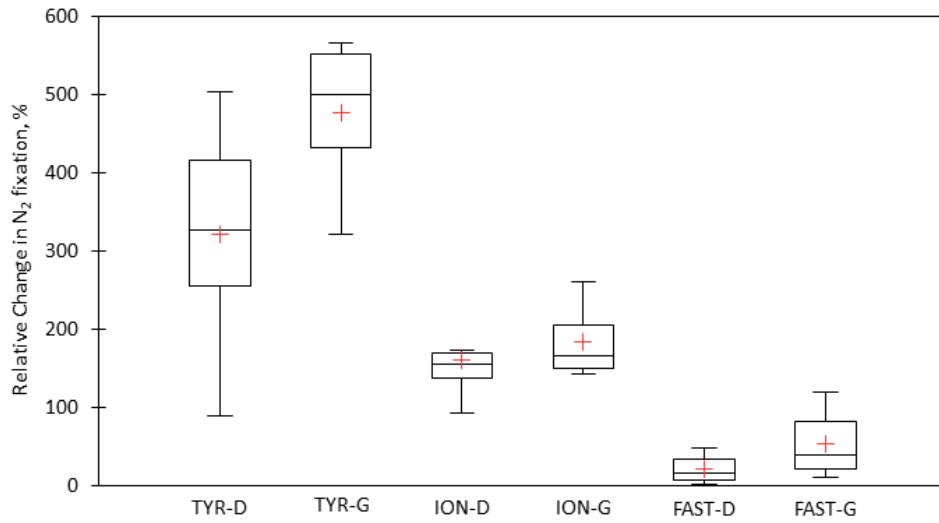


963
 964
 965
 966
 967
 968
 969
 970
 971
 972
 973
 974
 975
 976
 977
 978
 979

980 Figure 7: Box plots of the relative changes (in %) in N_2 fixation to the rates measured in the controls over the duration of the
981 dust seeding experiments (T1, T2, T3 or T4) at TYR, ION, and FAST stations. D means dust treatments under present
982 climate conditions (D treatment) and G dust treatments under future climate conditions (G treatment). The red cross
983 represents the average.

984

985



986

987

988

989

990

991

992

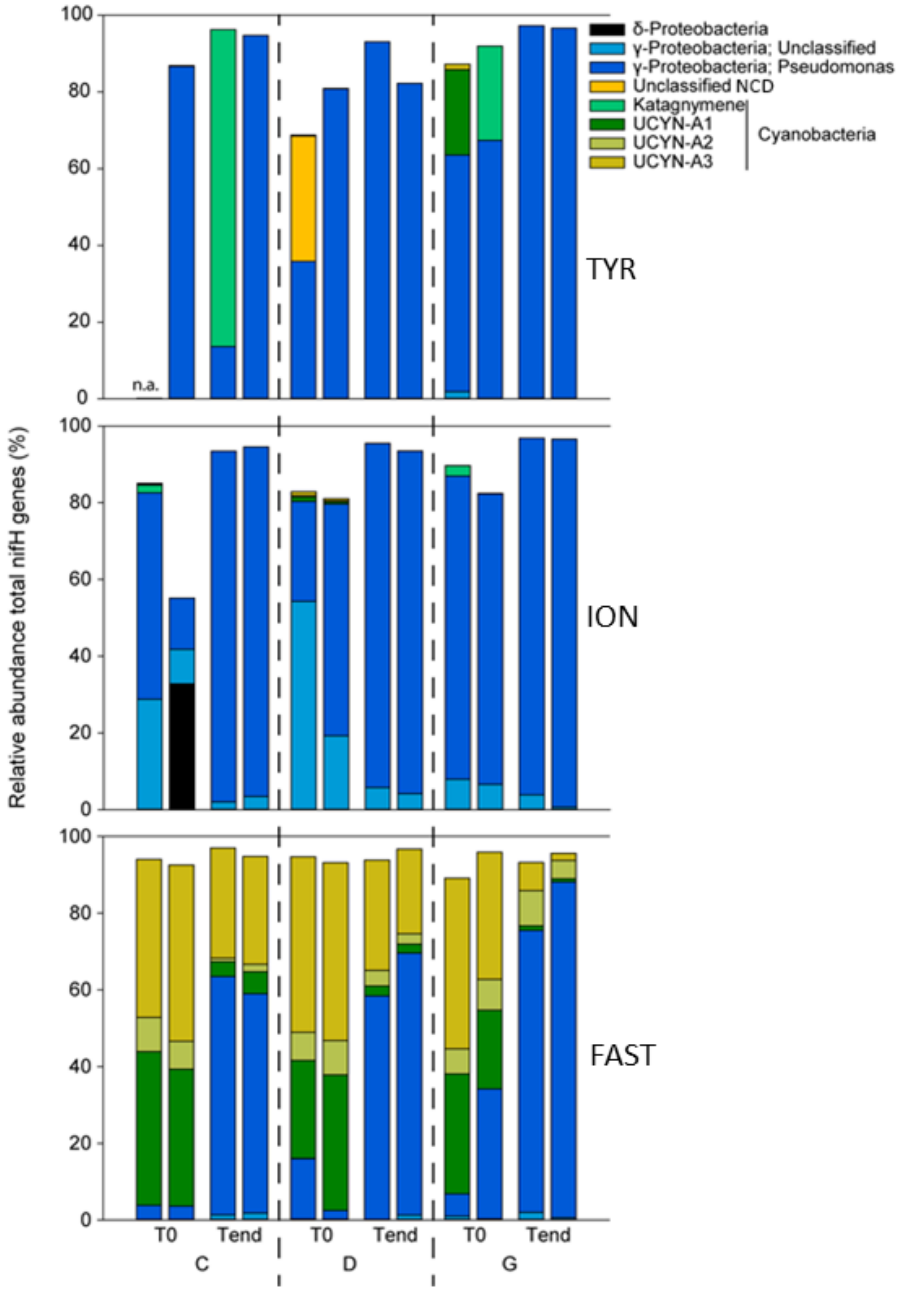
993

994

995

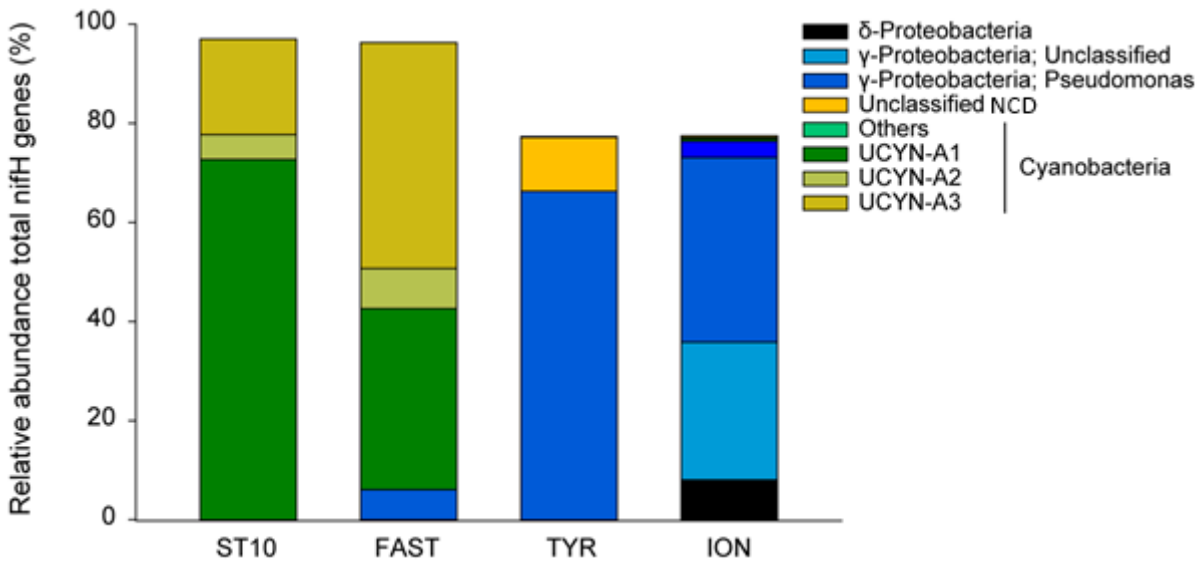
996

997 Figure 8: The composition of diazotrophs (based on 20 most abundant ASVs in the tanks) during the dust seeding
 998 experiments at the start (T0) and end (T3 at TYR and ION, and T4 at FAST) in each tank, at TYR (Top panel), ION (middle
 999 panel) and FAST (bottom panel). C1T0 at TYR was not included due to poor sequencing quality.
 1000



1001

1002 Figure 9: Relative abundance of the 20 most abundant nifH-ASVs in surface waters (values at TYR, ION and FAST are
 1003 based on average of duplicated control and dust treatments at T0).



1008
1009
1010
1011
1012
1013
1014
1015
1016
1017
1018
1019
1020
1021
1022